Natural Hazards
and Earth System
Sciences

Discussions

Open Access

EGU

Evaluation of Environmental Factors in Landslide Prone Areas of Central Taiwan using Spatial Analysis of Landslide Inventory Maps

Kui-Lin Fu[1], Bor-Shiun Lin[2,*], Kent Thomas[3], Chun-Kai Chen[4] and Hsing-Chuan Ho[5]

[1] Ph.D. Candidate, Department of Soil and Water Conservation, National Chung Hsing University

   Address: 145 Xingda Rd., South Dist., Taichung City 402

   TEL: (886-49) 234-7200 FAX：(886-49) 239-4306

   E-mail：fgl@mail.swcb.gov.tw

[2*] Principle Researcher, Disaster Prevention Technology Research Center, Sinotech Engineering Consultants, Taiwan.

   Address: No. 280, Xingu 2nd Rd., Neihu Dist., Taipei City, Taiwan, R.O.C., 11494.

   Corresponding author: TEL: (886-2) 8791-9198 EXT.309 FAX：(886-2) 8791-2198

   E-mail：bosch.lin@sinotech.org.tw

[3] Building Engineer – Infrastructure Services; Roads, Buildings and General Services Authority (BRAGSA).

   Address: Cnr. Lower Bay Street & McCoy Street, P.O Box 1100, Kingstown, St.Vincent and the Grenadines.

   TEL: (784) 430-0451 E-mail: kent.gary.thomas@gmail.com

 [4]Associate Researcher, Disaster Prevention Technology Research Center, Sinotech Engineering Consultants, Taiwan.

   Address: No. 280, Xingu 2nd Rd., Neihu Dist., Taipei City, Taiwan, R.O.C., 11494.

   TEL: (886-2) 8791-9198 EXT.307 E-mail：ckchen@sinotech.org.tw

[5] Associate Researcher, Disaster Prevention Technology Research Center, Sinotech Engineering Consultants, Taiwan.

   Address: No. 280, Xingu 2nd Rd., Neihu Dist., Taipei City, Taiwan, R.O.C., 11494.

   TEL: (886-2) 8791-9198 EXT.314 E-mail：hcho@sinotech.org.tw

Abstract

For many years the Shenmu watershed has been heavily impacted by landslides induced by extreme rainfall events, with an even greater impact in recent years due to climate change in addition to the Chi-Chi Earthquake after-effects. This study utilizes remote sensing technology to spatially and temporally interpret landslide processes in the Chushui and Aiyuzih sub-watersheds. An event-based landslide dataset is constructed which consists of 11 historical disaster events including 17 satellite images spanning the past 14 years. The study

Natural Hazards
and Earth System
Sciences

Open Access

Discussions

EGU

1   explores the contribution of causative environmental factors and other factors, which are

2   based on the physiographic conditions and geographic locations of the landslides induced, on

3   landslide potential. These factors are utilized to construct a logical reason-based rule set to

4   build a framework of procedures for semi-automated image interpretation and artificial image

5   identification.

6   Spatial relationships show that landslides are frequently found in areas at 1500m ~2000m of

7   elevation with slope gradient over 55% W-SE orientation, and within the Nanchuang

8   Formation adjacent to a 25m buffer zone of a river course in the Chushui and Aizuyih sub-

9   watersheds. Landslide occurrences are prevalent on both sides of the river course and are the

10   direct suppliers of sediments to the river, leading to sediment related disasters. Temporally, it

11   is found that the typhoon-induced landslides can be subdivided into three distinct time

12   intervals and the event that caused the greatest increase in landslide area can be recognized.

13   These intervals and their greatest impact events are as follows: (1) Before the 1999 Chi-Chi

14   earthquake, the 1996 typhoon Herb; (2) From the 1999 Chi-Chi earthquake to 2009 typhoon

15   Morakot, the 2004 typhoon Mindulle; (3) After this time period, the 2009 typhoon Morakot.

16   After comparisons were made of the total landslide areas and the new landslide areas before

17   and after the 1999 Chi-Chi earthquake in the two sub-watersheds, it was found that the

18   earthquake amplification effect of the quantified magnification was estimated to be at least a

19   doubling effect. This is an estimate that agrees well with the previous studies. The

20   methodology of our extensive study can be utilized to improve the dataset accuracy in similar

21   research, to classify and differentiate the contribution of environmental factors to landslide

22   occurrences and to build landslide occurrence potential maps for sub-watersheds. These

23   results are important to decision-makers to improve the reference information basis for

24   preliminary evaluation of the exposure of elements at risk. This, in turn, is important for

25   improving early warning systems, rapid response mechanisms, evacuation protocols and long

26   term mitigation solutions. The results may also influence the recommendations for

27   remediation of slope areas and construction of preventative engineering solutions in the two

28   sub-watersheds analyzed using the landslide potential map to prioritize urgencies by

29   comparing the necessity in one area to the next.

30   Keywords: Shenmu watershed, environmental factors, landslide potential map.

31

Natural Hazards
and Earth System
Sciences

Open Access

Discussions

1 Introduction

Since the 1996 typhoon Herb, Shenmu Watershed has experienced multi-temporal events such as the Chi-chi Earthquake, typhoon Toraji, typhoon Mindulle, typhoon Morakot, etc. These increased the landslide area in a watershed scale. Sediment production from bare and forested lands has tremendous impact on the objectives of preservation at downstream. Triggering factors are the primary contributors associated with the event which initiate or induce the slope failure or landslides, such as rainfall or earthquake events. Causative factors are the secondary contributors which increase the prevalence of landslide hazards, such as geology and distance from fault line. In some cases, causative factors may induce slope instability and failure such as rivers undercutting slopes and thus, can be classified as primary factors. This research primarily focuses on the causative factors in the Shenmu area. Long term monitoring of topographic changes was conducted via multistage satellite imagery of landslide areas to analyse landslide evolution and correlation to causative factors. Since the 1980s, many researchers have studied landslide evolution, correlation of causative/triggering factors to landslide zonation, landslide potential and probability using remote sensing technology (van Westen *et al.*, 2008). These studies joined local data with multistage DEM data generated by airborne and satellite-based optical sensors to monitor topographical evolution and landslide activity of high-mountain terrain deformation, to collect causative/triggering factors data and to compare their contribution to landslide events which can be utilized for early warning of hazards and reduction to disaster risk (Carrara, 1992、1999；Montgomery and Dietrich, 1994). Kääb (2002) and Chau *et al.* (2004) estimated the landslides zonation and population at risk according to landslide susceptibility map that quantifies hazard-inducing factors such as elevation, slope gradient, rock characteristics, debris deposits, population distribution, climate and rainfall. Metternicht *et al.* (2005) conducted long-term monitoring of landslide hazards, deployment of landslide database, and studies of hazard-inducing factor correlation in Sweden. Barlow *et al.* (2006) illustrated correlation between landslide and environmental factors by quantifying the characteristics of mass movement and determining based on normalized differential vegetation index (NDVI) and terrain slope gradient. Bai *et al.* (2009) utilized landslide-triggered factors to establish the landslide susceptibility map for the Three Gorges Dam in the Yantze River. Mehrnoosh *et al.* (2009) established a landslide potential map which demonstrates that the primary landslide-

Natural Hazards
and Earth System
Sciences

Discussions

Open Access

EGU

1   triggered factor is formation lithology and also concluded that soil profile as well as human

2   development is only secondary.

3   In Taiwan, Chen and Cheng (1997) used three periods of SPOT satellite images of the

4   Fungshan river watershed combined with GIS to quickly extract the evolution data from large

5   hillslope development within the watershed to effectively monitor land use change and

6   vegetation coverage evolution within the watershed. The National Science and Technology

7   Center for Disaster Reduction (2004) used satellite images of post typhoon Aere event to

8   digitize and calculate the incremental landslide area in Shihmen Reservoir watershed to

9   conduct research on correlation among landslide size, landslide zoning, human activity,

10   accumulated rainfall, etc.. Taiwan Soil and Water Conservation Bureau (SWCB, 2010[a])

11   reported that typhoon-induced landslide areas within Shih-men Reservoir watershed are

12   concentrated between 1,000m to 1,500m, mostly on slopes steeper whose geology mostly

13   belongs to Taliao Formation.

14   For effectively evaluating causative factors of landslides, this study compiles all the historical

15   satellite images of the Shenmu watershed and uses a proposed framework for semi-automated

16   image interpretation and artificial image identification procedures which systematically

17   improves the quality of data content and data structure so that it can definitely promote data

18   integrity and accuracy for improving value and reliability of landslide inventory with pre and

19   post various triggering events, meteoric, seismic and environmental. Secondly, using spatial

20   analysis with GIS-based program can explore or extract environmental factors of the collected

21   spatial data layer and DEM materials to qualify and construct such potential maps. Finally,

22   these results would help decision-makers to improve the reference information to forecast the

23   occurrence of future landslide basis for preliminary evaluation of the exposure of elements at

24   risk. This in turns would be important for improving early warning systems, rapid response

25   mechanisms, evacuation protocols and long term mitigation solutions.

26   **2   Hazard History of Study Area**

27   Shenmu watershed is situated in the southwestern corner of Xinyi Township in Nantou

28   County. Traffic access mainly depends on the Highway 21 which goes north to Shueilee

29   Township. Shenmu watershed is highly mountainous with steep slopes. Local topography is

30   characterized by tall mountains and steep slopes, with elevations ranging from 500 m a.s.l. to

Natural Hazards
and Earth System
Sciences
Discussions

1   2500 a.s.l. and slopes which are steeper than 28.8° represent 45% of the total regional

2   extension (72.16 km^2) and 47.75% of the slopes are north facing (Ho *et al*., 2011; Lo *et al*.,

3   2012). The Shenmu watershed is crossed by three primary geologic structures: the northeast-

4   southwest Heshe Anticline and Tungfu Syncline and the Chen-yo-lan River Fault. These

5   mountain slopes are covered with dense forests and were built up by the Nanchuang and

6   Heshe formation (see Fig. 1). These formations consists mainly of hard, dark grey argillite

7   and grey slate with thinly bedded muddy sandstone, which are prone to severe weathering and

8   become weak layers in the rock strata. The Shenmu watershed is located in the Heshe river

9   watershed, an upstream watershed of the Chen-yo-lan river. The Aiyuzih, Housha and

10 Chushui rivers constitute the Heshe river watershed. Temperature ranges from 5.9℃ ~ 14.4℃,

11 averaging 10.9 ℃ annually. The average annual accumulated rainfall for three weather

12 monitoring stations located at Alishan, Shenmu Village, and Hsinkaoko ranges from 1,950 to

13 4,980mm.

14 In 1996, typhoon Herb brought lots of rainfall up to 714 mm over 3 days that causes the first

15 occurrence of massive landslide. Chushui and Aiyuzih rivers, which are in upstream portion

16 of the Shenmu watershed, deliver massive amount of sediment material which converged and

17 flowed toward the mid and downstream of Heshe River. Consequently, Shenmu Elementary

18 School which was near the converging point was buried by the debris, and the checkpoint and

19 Shenmu Bridge were both destroyed. The total out-flowing debris was 450,000 m^3. Thereafter,

20 in May 1998, the Hosa River Bridge in front of Shenmu Elementary School was destroyed by

21 the debris flow from Chushui River. 155 people from 39 households were stranded, causing

22 large scale panic and forcing nationwide attention to debris flow hazards. Similarly, in May

23 1998, the plum rain season (i.e. in the East Asia region, it coincides with the season of plums

24 ripening) carried massive rainfall which caused the Hosa River Bridge to be destroyed by

25 debris flow so that over 100 residents were isolated. The 2001 typhoon Toraji brought

26 accumulated rainfall of 517mm, and the rehabilitated Hosa River Bridge was once again

27 destroyed. Highway 21 access was disrupted and there was extensive damage to housing and

28 farms. Between May and June 2004, Shenmu Watershed had four debris flow events due to a

29 series of continuous rainfall events. This caused the groundsill structures deployed by the

30 Taiwan Forestry Bureau at upstream Aiyuzih River to be buried, causing severe sediment

31 material on the two sides of river flank. In July of the same year during typhoon Mindulle

Natural Hazards
and Earth System
Sciences

Open Access

EGU

Discussions

1   whose total accumulated rainfall was up to 1,254 mm, there was large-scale landsliding at

2   upstream Aiyuzih River and large amount of sediment material deposited in the river course.

3   In June 2006, two days of non-stop rainfall brought 1,332 mm of accumulated rainfall to

4   Shenmu watershed. Chushui River once again had debris flows and large-scale landsliding

5   that damaged cultivated farmland. On August 6th, 2009, typhoon Morakot gradually passed

6   through Taiwan. Its intensity steadily increased and continued to move to the west. Typhoon

7   Morakot had a complete structure and moved slowly with accumulated rainfall duration of six

8   days (2009/08/05~08/10). Also, on the night of August 8th, the system's accumulated rainfall

9   reached 900 mm which exceeded the 200-year rainfall return period. This caused the river to

10 surge, severe scouring on the two flanks, several collapses on the roads and massive sediment

11 washed down destroying the downstream Aiyuzih Bridge. The disaster points of this event are

12 investigated as shown in Figure 2. Consequently, Shenmu Watershed almost was like an

13 isolated island without communications and local residents had a rescue and less resource

14 supply for livelihood. In a view of above the disaster history, Shenmu area is generally

15 affected by debris flows during the typhoon and flood seasons and has the highest debris flow

16 frequency throughout Taiwan, especially within Chushui and Aiyuzih subwatersheds.

17 This study aims to analyze the rainfall event-induced and environment factors correlated with

18 landslide evolution of Chushui and Aiyuzih subwatersheds to serve as a reference for disaster

19 prevention and management.

20 **3   Spatial Data and Methodology**

21 Rapid advances of computer technology have promoted similar improvements in remote

22 sensing (RS) techniques and geographic information systems (GIS). Multi-stage RS images

23 can be effectively applied to practical issues such as landuse planning and mapping, detection

24 of geomorphological change and wide-area disaster monitoring. Also, in terms of efficiency

25 and cost, remote sensing is superior to traditional methods especially for collecting and

26 processing data over large areas. Hazard zonation is the fundamental basis of all modern

27 disaster management and preparedness strategies and provides a basic knowledge of potential

28 danger of specific events in a given area. Remote sensing has proven to be very effective in

29 performing rapid, emergency data collection during post disaster recovery periods. As a result,

30 countries around the world are increasingly using remote sensing to perform prompt large-

31 scale post-event natural disaster surveys. Van Westen (2000) has pointed the interpretation of

Natural Hazards
and Earth System
Sciences
Discussions

Open Access

EGU

1   post-event residual characteristics, such as landslide scars, interpreted and confirmed using

2   RS and field investigation studies then consolidated into GIS databases create the foundation

3   of hazard zonation. Other authors have further suggested improvements to hazard zonation by

4   including various other datasets, such as borehole data, geological data, knowledge derived

5   from local communities and past events (Fell *et al.*, 2008). These hazard maps should provide

6   local authorities, communities, decision-makers and stake-holders (such as private companies

7   and NGOs) with comprehensible information which can be utilized for planning. Van Westen

8   et al. (2008) have also suggested that longterm RS data, GIS data and satellite imagery

9   projects can further enhance hazard mapping by providing spatial and temporal relationships

10   which map the variability and evolution of geomorphological, environmental and agricultural,

11   river, man-made development and settlement datasets. The issue faced by many countries is

12   the lack of longterm data, cost of longterm projects and the seeming lack of short term

13   benefits. These GIS-based information and datasets when adequately utilized can be

14   organized into easily accessible disaster management systems to improve disaster response,

15   create early warning/detection systems, utilized for probalistic research and subsequent long

16   term data analysis purposes, and finally to further enhance the disaster mitigation and

17   prevention stages of the disaster management cycle.

18   In this study, the object-oriented Trimble® eCognition Developer has been used to handle

19   image analysis tasks, to process a variety of image sources, to provide automatic or semi-

20   automatic processing and analysis. It is also used in mapping landslide studies after a given

21   landslide event to develop rule sets for the analysis of remote sensing data (Borghuis *et al.*,

22   2007; Joyce *et al.*, 2008; Lu *et al.*, 2011). eCognition Developer enables non-technical users

23   to configure, calibrate and execute image analysis workflows (Trimble, 2010). For landslide

24   detection, eCognition Developer has specific characteristic for classifiying polygon object

25   instead of grid-based information. It can execute image segmentation quickly and easily in

26   different scale under supervised classification and using fuzzy logic classification algorithms

27   to improve overall accuracy of classified results for a specific event.

28   In term of spatial and statistical analysis, the landslide inventory gives insight into the

29   location of landslide phenomena in a specific study area, displaying information on landslide

30   activity (van Western *et al.*, 2008), and therefore should require multi-temporal landslide

31   information for specific disaster-prone regions. The occurrence of landslide in a watershed

Natural Hazards
and Earth System
Sciences

Open Access

EGU

Discussions

1 scale area is directly related to the rainfall distribution, accumulation, duration, hourly

2 intensity, and its patterns, but is also affected by environmental conditions. Many studies have

3 focused on the spatial analysis of landslides affected by environmental factors including

4 morphology, geology, hydrology, geomorphology and human activities (Cruden and Varnes,

5 1996; Aleotti and Chowdhury, 1999; Ayalew and Yamagishi, 2005). Especially, rainfall is the

6 primary factor triggering landslides in Taiwan, and can also be used as a key factor in

7 predicting where and when landslides will occur (Chen et al., 2014). Several studies show

8 rainfall event characteristics, such as rainfall duration, rainfall intensity, accumulated and

9 antecedent rainfall could be quantified as the threshold value for landslide occurrence (Caine,

10 1980; Crozier, 1986; Jakob and Weatherly, 2003; Chen *et al*., 2014). Chen et al. (2014) have

11 observed that the 1999 Chi-Chi earthquake and the accumulated rainfall of subsequent

12 typhoons and heavy rainfall events substantially affected the distribution and severity of

13 landslides in the Shenmu watershed.

14 In view of the above, the following sections would exhaustively express our spatial data,

15 utilized methodology and proposed procedure to evaluate environmental factors in landslide

16 prone areas of Central Taiwan using spatial analysis of landslide inventory maps.

3.1 Landslide Inventory Maps

18 To build a reliable hazard map to predict landslide-prone areas in Shenmu Watershed, this

19 study required a landslide inventory that is as complete as possible in both space and time

20 (Glade, 2001; Malamud *et al*., 2004; van Westen et al., 2008). This study establishes the

21 event-based landslide inventory using multi-stage satellite imagery interpretation for Chushui

22 and Aiyuzih subwatersheds in the Shenmu area. Image interpretation defines the

23 physiographic and geographic nature of area as environmental parameters. These

24 environmental parameters are joined with the rainfall triggering factors to correlate landslide

25 proneness. A collection of landslide inventory maps of extreme meteorological events and one

26 extreme earthquake event (Dadson *et al*., 2003; Lin *et al*., 2008) affecting the Shenmu area is

27 built containing 11 events from 1996 to 2009 including 1996 typhoon Herb, 1999/5/28 heavy

28 rainfall, 1999 Chi-Chi earthquake, 2001 typhoon Toraji, 2004 typhoon Mindulle, 2008

29 typhoon Kalmaegi, typhoon Fung-wong, typhoon Sinlaku, typhoon Jangmi, 2009 typhoon

30 Morakot and typhoon Parma. (see Fig. 3 and Table 1).

Natural Hazards
and Earth System
Sciences

Open Access

Discussions

EGU

1 Landslide inventory maps are the key component to correlate environmental parameters with

2 triggered factors and changes in these characteristics after major triggering events (Coe *et al*.,

3 2004). Using satellite remote sensing data for the identification and mapping of small-scale

4 landslide areas has been improved substantially over the last decade. The selection of satellite

5 imagery sources is an important factor affecting the reliability of identification, satellite

6 imagery for later events has higher spatial resolution due to more advanced technology of

7 satellite data acquisition system. SPOT-series satellite has been widely utilized where

8 landslides without vegetation can be differentiated spectrally from their surrounding areas

9 (Yamaguchi *et al*., 2003; Nichol and Wong, 2005; Borghuis *et al*., 2007). Accordingly, for

10 pre-2004 imagery this study adopted SPOT1-SPOT4 satellite imagery whose resolution is

11 6.25m or 10m and for post-2004 imagery this study has adopted SPOT5 satellite or

12 FORMOSAT II satellite imagery whose resolution is 2.5m and 2.0m for completion of 1996-

13 2009 landslide inventory maps (see Fig.4). Besides, all of the satellite imagery data qualities

14 are required to be low or no-cloud cover, and the capture angle of satellite data acquisition

15 system is less than 15 degree (SWCB, 2010[b]). Table 2 lists the adopted image data source for

16 each event. This study, using GIS-based layers of the landslides inventory maps caused by

17 extreme events and of different physiographic characteristics of the study area, discusses the

18 long term changes in the Shenmu watershed and explores the correlation between

19 environmental parameters and landslide area.

20 **3.2 Image Interpretation and Identification Procedure**

21 Numerous studies have elucidated the effects of subjective judgment errors made by landslide

22 researchers using semi-automated methods (Martha *et al*., 2010). In modern landslide

23 research, the most common approach to landslide inventory mapping is using remote sensing

24 technology combined with GIS-based programs. This study adopted object-oriented semi-

25 automated image interpretation to quickly extract temporal changes from pre- and post-

26 disaster satellite imagery in areas which have been affected by landslides. Then, all of the

27 extracted areas were filtered out and error-checking was carried out through elaborate

28 artificial quality control for completing data standardization and promote data accuracy.

Natural Hazards
and Earth System
Sciences

Discussions

Open Access

EGU

1 3.2.1 Semi-automated Image Interpretation

2 The suggested object-oriented semi-automated image interpretation procedure (see Fig.5) in

3 this study will be organised into four steps described as follows:

4 a. Import satellite images and reference layer：Before importing the whole inventory of

5   satellite images into this program, the priority action is required to define the local

6   characteristics of landslide area within satellite images depending on some GIS-based

7   reference layers such as road, landuse and DEM-derived slope or aspect for effectively

8   detecting object likely landslid-shape polygons.

9 b. Optimize object scale size：The imported satellite images are separated regularly by

10   multi-resolution segmentation method, which for a given number of image objects,

11   minimizes the average heterogeneity and maximizes their respective homogeneity into

12   different object size from small to large scale. If the scale size is too small, large amount

13   of objects are separated and too fractured. The same thing would be composed of

14   multiple objects and that would cause subsequent increase in processing time. Conversely,

15   if the scale size is too large, the separated objects are too few that can not divided to be

16   the proper objects for classification which means landslide are hardly detected.

17   Consequently, one shoud set up minimum map unit be greater than 9 to 12 pixels

18   (Desclée et al., 2006) to optimize object scale size based on the best resolution of SPOT-

19   series satellite images in practical application.

20 c. Construct the appropriate classified rule set for landslide detection：when completeing

21   object scale size optimization, the appropriate classified rules for landslide detection need

22   to be systematically constructed. Users should establish feature categories of classification

23   and hierarchy of the tree structure, such as landslide, buildings, road, rice fields,

24   vegetation, river systems, cloud, etc.. Then, it would help to detect the above features

25   based on its logical rule set developing on its own characteristics. In this study, the

26   adopted SPOT-series satellite images has spectral bands, with simultaneous panchromatic

27   and multispectral acquisitions, whose R, G and NIR spectral bands refer to Normalized

28   Difference Vegetation Index (NDVI) for distinguishing non-vegetated area in satellite

29   imagery (Lambin and Strahlers, 1994; Tsai et al., 2010). If NDVI value is less than 0.05,

30   there is a high probability that the detected land cover/objects are landslides (see Fig.5). In

Natural Hazards
and Earth System
Sciences

Open Access

Discussions

EGU

1   addition, the DEM-derived slope for a given area is used to automatically classify and

2   delineate non-landslide polygons, where slope gradient is less than 5%, and likely-

3   landslide polygon. Expert judgement is designated artificially as a logical ruleset to

4   increase the precision of detection of landslide distribution in a temporal and spatial scale.

5   d. Export classified polygon objects：Classified landslide polygon objects are exported into

6   GIS-based program as in SHP layer format which include attached information such as

7   classification attributes, area, aspect ratio, etc., for further artificial checkup, identification

8   and error elimination.

9   **3.2.2 Artificial Image Identification**

10 Artificial image identification procedure refers to interactively adjusting the classified

11 landslide polygon objects based on visual interpretation with professsional experience,

12 historical information, aerial photos, land use/land cover and landslide inventory dataset under

13 the GIS-based program (Tsai *et al*., 2010) such as ArcGIS and Mapinfo. The purpose of this

14 procedure aims to ensure or promote the overall accuracy of classified reuslts for a specific

15 event which identify the boundaries of landslide polygons if corresponding with land use and

16 land cover of current geomorpological environment. Similar to the previous section, the

17 artificial image identification procedure (see Fig.5) will conform to the following two steps as

18 described below:

19 a. Initial image identification：

20   This step depends on professional staff with associate geomorphology knowledge and

21   long-term experience in visual landslide interpretation. Often, some parts of satellite

22   images may have ambiguities along the boundaries of landslides, especially near existing

23   stream channels, clouds or shadows in the images that would cause omission of landslide

24   polygon objects (Tsai *et al*., 2010). For solving this problem, the staff uses aerial photos

25   and pre-event or post-event images as reference layers to identify if all of landslide

26   polygon objects have been delineated to minimize the probability of omission.

27 b. Advanced image identification：

Natural Hazards
and Earth System
Sciences

Open Access

Discussions

EGU

1 After intial image identification, some objects belong to artificial agricultural lands or

2 man-made croplands including bamboo field, tea or vegetable garden. In satellite imagery,

3 Agricultural croplands and crops which have been cleared (leaving exposed areas) have a

4 hue that is close to the landslide polygon object and this can cause judgment confusion in

5 the intial image identification. Therefore, this step utilizes landslide inventory dataset or

6 land use/land cover map to eliminate the identified landslide polygon objects and

7 diffrentiate the agricultural croplands for final quality control to reduce the error from the

8 semi-automated image. Finally, the identified landslide polygon objects is doubly

9 examined thoroughly to establish a complete landslide inventory map for correlation

10 analysis with multi-stage landslide inventory maps.

11 ### 3.3 Spatial and Statistical Analysis

12 The selection of specific environmental factors, which is sometimes referred to as causative

13 factors, in a given region will strongly dominate the probability for forecasting the occurrence

14 of future landslide. In this study, using spatial analysis with GIS-based program can explore

15 or extract environmental factors of the collected spatial data layer and DEM materials (such

16 as elevation, slope, aspect, geology and roads, etc.) (see Fig.6) overlapping the established

17 complete landslide inventory map for specific each event. Among these factors of

18 geomorphological information, a collected high-resoultion DEM was used to calculate/

19 generate elevation, slope and aspect maps under GIS analysis tools by an interpolation

20 method. Finally, the above environmental factors were analyzed to identify mutual

21 correlations with the landslides for a given event and it also can be used to account for the

22 main cause of landslide and illustrate disater-prone zoning map for effective watershed

23 management, planning of disaster prevention works and reducing risk of landslide hazards

24 during the flood season.

25 To effectively appreciate rainfall-triggered events that cause landslide occurrence affecting

26 the evolution of landforms and severe topological changes in Chushui and Aiyuzih

27 subwatersheds within study area, this study compiles satellite images from 12 historical

28 hazard events from the 1996 Herb to 2009 Parma (see Table 1 and Table 2). According to the

29 suggested image interpretation and identification procedure, the landslide inventory of both

30 pre-event and post-event has been detailed mapped into a reliable spatial database. Afterward,

Natural Hazards
and Earth System
Sciences

Discussions

EGU

1   this study estimated possible correlation between landslides and the above mentioned

2   environmental parameters and connecting landform evolution related to disasters by

3   performing GIS spatial and statistical analysis to illustrate a series of frequency

4   distribution/histogram or statistical results for each event. The detailed spatial and statistical

5   analysis process in this study are illustrated in Fig.6 and the adopted categories of

6   environmental factors are clearly lised in Table 3.

7   **3.3.1 Landslide analysis with enviromental facator**

8   Event-based landslide evolution study compiles the pre- and post-event total landslide areas

9   and new landslide areas which affected the study area and the corresponding landslide ratio

10 (*LR*) and new landslide ratio (*NLR*) for a given watershed scale as determined by the landslide

11 inventory database (Malamud *et al*., 2004; Lin *et al*., 2008; Chang *et al.*, 2014). Pre-event

12 total landslide areas demonstrate the pre-event stability conditions and represents zones which

13 further landslide evolution may occur or zones which suffer from wide-scale stability issues.

14 Post-event total landslide areas demonstrate post-event stability conditions of the study area

15 and represents both the historical landslides and those landslides formed after or during the

16 event. New landslide areas represents the difference of these two and denotes the landslides

17 directly caused by the event. Some researchers (Chen and Wu, 2006; Chang *et al*., 2007; Lin

18 *et al*., 2008) used the landslide ratio and new landslide ratio after an event to analyze landslide

19 condition. The landslide ratio is defined as the ratio of the total landslide area to the given

20 watershed area. Similarly, the new landslide ratio as the ratio of new landslide area to the total

21 landslide area. For evaluating environmental factors contribution to landslide evolution, the

22 above related terminology would be defined accordingly and the schematic layout and its

23 corresponding explanations are also shown in Fig. 7. The two mentioned ratio equations can

24 be expressed in percentage respectively as follow:

25 $$LR(\%) = \frac{TLA}{WSA} \qquad (1)$$

26 Where TLA is a total landslide area after one specific event including the old landslide area

27 and new landslide area; the old landslide area is referred to the landslide already exists before

28 that event; new landslide area is referred to be appeared only after that event; WSA is a given

29 watershed area.

1    $$NLR(\%) = \frac{ILA}{WSA}$$ (2)

2   Where ILA is a toal new landslide area after the specific event.

3   On the other hand, it is an alternative purpose for rigorously understanding the impact of

4   environmental factors (see Table 3) on historical rainfall event-triggered landslide inventory

5   maps, and also evaluate the relationship between the toal landslide area and each single type

6   or classifications of the same condition. So, this study uses conditional analysis mehtod

7   (Carrara *et al*., 1995; Clerici *et al*., 2006) under GIS-based program incorporate with spatial

8   and statistical analysis for studying on the landslide contribution from a number of causative

9   fators existed simultaneously. Clerici *et al*. (2006) studied how factors can be directly or

10   indirectly related to landsliding by adopting a method of representing factors as a number of

11   data layers in overlayed order to obtain all the possible combinations of the various classes of

12   the different factors. The concept of unique condition units (UCU), unique condition subareas

13   and unique condition classes have been used by different researchers to represent terrain units

14   compiling the combinations of environemntal factors (Bonham-Carter, 1994; Chung *et al*.

15   1995). Landslide contribution of environment factors are then obtained in each UCU. A

16   general assumption used in landslide research is that the conditions which have led to

17   landslide occurence in the fact are the likely conditions which will lead to future instability

18   and landsliding. The computed landslide contribution represents causative factors occupied

19   area entailing with landslide in percentage. Formally, the landslide contribuion (LC) is

20   redefined as (Carrara *et al*., 1995; Clerici *et al*., 2006):

21   $$LC(\%) = \frac{TLA \cap UCUA}{TLA}$$ (3)

22   Where $UCUA$ means the total area of unique condition unit (UCU).

23   The study uses the above conceptual equation to assess landslide contribuion of each UCU to

24   the corresponding environmental condition. The landslide contribution of UCU represents the

25   degree of influence of any causative factors. Among them, if the contribution extent is high,

26   this means in the classification, it is a main causative factor which would help verifying where

27   the main disaster-prone area regarding the assessment of landslide presence, the choice of the

28   factors to use in the analysis and the evaluation of the reliability of the resulting zonation. All

29   of the detailed results will be discussed in the following sections.

1   **3.3.2 Landslide analysis with rainfall events**

2   Researchers suggest using aerial photo and satellite images to interpret the landslide area to

3   reduce investigation cost. In terms of methodology, there are empirical formula, expert

4   judgment, mechanism approach, and statistical approach (Uchihugi, 1971；Montgomery and

5   Dietrich, 1994；Aleotti, 2004). Among them, empirical formula is most widely used.

6   Uchihugi (1971) used rainfall data from different regions to obtain the formula for

7   accumulated rainfall and landslide ratio. SWCB (2010[a,b]) used Uchihugi's empirical model to

8   quickly obtain disaster sediment production in the watershed. This was compared with the

9   observed data by airborne LiDAR, and results from watersheds with higher rainfall station

10   density were a closer match.

11   Uchihugi (1971) targeted new landslides in typhoon events for analysis. He discovered that

12   the greater the accumulated rainfall, the larger and more numerous the landslides. Uchihugi

13   adopted the analytical concept and used rainfall data from different regions. The relationship

14   between accumulated rainfalls and landslide area ratio was obtained to simplify and speed up

15   the estimation of new landslide areas. However, when the rainfall parameters of Uchihugi

16   empirical model reach the critical rainfall, the new landslide in the watershed becomes zero.

17   This does not fit with the physical reality. The study extended from Uchihugi concept on the

18   basis that when the watershed accumulated rainfall equals critical rainfall, landslide should

19   happen. Therefore, it included a parameter for initial new landslide ratio, which is the state of

20   landslide when the watershed is under critical rainfall. According to Eq. (2), Uchihugi

21   formula was modified as below:

22   $$NLR(\%) = \frac{ILA}{WSA} \approx C + K \times 10^{-6}(R_A - r)^2 \ RI \geq r \qquad (4)$$

23   Where K is the coefficient and R_A is the accumulated rainfall of an event (mm). r is the

24   critical rainfall for landslide initiation (mm), and C is initial increment landslide ratio when

25   the critical rainfall triggers the landslide.

26   Due to lack of actual critical rainfall (r) for landslide in this study area, the critical rainfall (r)

27   could be assumed as 200 mm based on the studied results of rainfall data analysis for Shenmu

28   area from Lo *et al*. (2012). The above formula indicates that only accumulated rainfall of the

29   watershed is necessary to estimate the total of the new landslide area. Therefore, it is the key

Natural Hazards
and Earth System
Sciences
Discussions

1   to rainfall distribution characterization in typhoon events and data accuracy. It also affects the

2   regression analysis reliability. This study adopted Uchihugi formula to analyze correlation

3   between event-based landslides inventory and associated accumulated rainfall with its

4   corresponding new landslide ratio for predicting landslide magnitude in the future.

5   **4   Results**

6   This section utilized a dataset of complete and reliable landslide inventory maps of Shenmu

7   area from the 1996 Herb to 2009 Parma through the suggested image interpretation and

8   identification procedure which have edited and filtered out any possible error area for further

9   minimizing omissions. Also, it would help to effectively grasp the total landslide area and

10 new landslide area caused by an event in the study area and deeply explores the relative

11 relationship between landslide inventories and the environmental factors or rainfall events

12 with its corresponding accumulated rainfall. The main purpose of this analysis can be

13 concluded as:

14 a. Temporal analyses: Using complete landslide inventory maps of the Shenmu area to

15   represent continuous landslide change with time subjected to each typical typhoon events

16   especially for most landslide-proneness of Chushui and Aiyuzih subwatersheds and also

17   recognize which event dominates maximum landslide area in the disaster history. In

18   addition, the range of the maximum and minimum landslide area would be constructed

19   based on the above analyzed results, which will help to quickly assess the effects of

20   landslide changes in the environment of an event in the future, whether or not fall within

21   acceptable limits to avoid landslide risk.

22 b. Spatial analyses: Using spatial and statistical analysis with environmental factors or

23   rainfall events with its corresponding accumulated rainfall to find main landslide

24   contribution of each disaster events and next elaborate a combination of causative factors

25   for any given area within the study area. According to a combination of causative factors ,

26   one could develop a set of reason-based rules for preliminary delineation of potential

27   landslide area focusing on areas which have well-vegetated land cover and presently have

28   no evidence of landslide activity and situated at stable condition to lower damage loss of

29   disaster and implement rapid response and urgent decision-making during disaster.

Natural Hazards
and Earth System
Sciences
Discussions

Open Access

1   As the above mentioned, this study completed the landslide analysis of Chushui and Aiyuzih

2   subwatersheds based on the Eq. (1) to Eq. (4) to represent the characteristic of spatial-

3   temporal distribution of landslide.

4   **4.1   Temporal Landslide Distribution**

5   Landslide distribution of Chushui and Aiyuzih subwatershed (see Fig. 8~9) in temporal scale

6   are separated into three periods to discuss typhoon/heavy rainfall-induced disaster magnitude

7   and its change after earthquake event.

8   **(1) Chushui subwatershed**

9   a.   pre-1999 Chi-Chi earthquake events:

10   Before 1999 Chi-Chi earthquake, Chushui subwatershed had been subjected to extreme

11   rainfall events including 1996 typhoon Herb and 1999/5/28 heavy rainfall which caused

12   numerous landslide areas in the upstream watershed (Chen *et al.*, 2014) as shown in Fig. 10.

13   For landslide distribution in Chushui subwatershed during pre-1999 Chi-Chi earthquake

14   period, it is found that total landslide area ranged from 3.148 to 16.164 ha and its

15   corresponding *LR* is 0.365% to 1.876% before 1999 Chi-Chi earthquake. And, the new

16   landslide area caused by each event ranged frome from 9.372 to 13.973 ha and its

17   corresponding *NLR* is 1.088% to 1.622%. In this period, the study found that most landslide

18   area and its distribution was strongly affected by typhoon Herb (see Fig. 10) which brought

19   the highest accumulated rainfall up to 879mm with prolonged duration and also led to

20   frequent debris flow occurrence.

21   b.   from1999 Chi-Chi earthquake to pre-typhoon Morakot events

22   In this period, Chushui subwatershed had been subjected to extreme rainfall events including

23   2001 typhoon Toraji, 2004 typhoon Mindulle, 2008 typhoon Kalmaegi, typhoon Fung-wong,

24   typhoon Sinlaku, typhoon Jangmi which reactivated old landslide areas and activated new

25   landslide areas in the upstream watershed as shown in Fig.10. For Landslide distribution of

26   Chushui subwatershed in the period between 1999 Chi-Chi earthquake and pre-typhoon

27   Morakot events, it is observed that total landslide area ranged from 14.465 to 57.196 ha and

28   its corresponding *LR* is 1.679% to 6.639%. And, the new landslide area caused by each event

29   ranged from 3.918 to 35.987 ha and its corresponding *NLR* is 0.455% to 4.177%. In this

Natural Hazards
and Earth System
Sciences

Discussions

EGU

Open Access

1   period, one finds that most landslide area and its distribution are caused by 2004 typhoon

2   Mindulle (see Fig. 10). Then, compared this period with the previous, the amount of total

3   landslide and new landslide area after 1999 Chi-Chi earthquake is at least increased by 3.53

4   times and 2.57 times approximately. This fact implies that the main cause of the expanding

5   landslide area was the disturbance of geomaterial by strong earthquakes with giant seismic

6   shaking force (Lin *et al*., 2008).

7   c. post-typhoon Morakot events

8   In this period, Chushui subwatershed had been subjected to extreme rainfall events including

9   2009 typhoon Morakot and typhoon Parma. For landslide distribution of Chushui

10   subwatershed in post-typhoon Morakot events period, it is observed that total landslide area

11   ranged from 69.381 to 72.529 ha and its corresponding LR is 8.053% to 8.418%. And, the

12   new landslide area caused by each event ranged from 5.618 to 30.983 ha and its

13   corresponding NLR is 0.652% to 3.596%. Typhoon Morakot brought unpredictable

14   accumulated rainfall (2,099.5mm) with prolonged duration and high hourly intensity, this

15   event stuck in Chushui subwatershed and triggered many landslides including some large-

16   scale landslide over 10 ha and also caused debris flow occurrence and natural dams which

17   resulted in biggest manigtude of total landslide area within its disaster history.

18   **(2) Aiyuzih subwatershed**

19   a. pre-1999 Chi-Chi earthquake events

20   Before 1999 Chi-Chi earthquake, Aiyuzih subwatershed had been subjected to extreme

21   rainfall events as the same as Chushui subwatershed as shown in Fig.xx. In this period, total

22   landslide area ranged from 10.091 to 17.575 ha and its corresponding LR is 2.519% to

23   4.387% before 1999 Chi-Chi earthquake. And, the new landslide area caused by each event

24   ranged frome from 5.167 to 10.175 ha and its corresponding NLR is 1.290% to 2.540%. It is

25   obviously inferred that that most landslide area and its distribution was deeply affected by

26   1998/5/28 heavy rainfall (see Fig. 11) which does not coincide with the typical event of

27   Chushui subwatershed. Also, the total landslide area of Aiyuzih subwatershed in this period is

28   slightly over Chushui subwatershed about 2.275 ha even if Aiyuzih subwatershed area is

29   smaller than Chushui subwatershed.

30   b. from1999 Chi-Chi earthquake to pre-typhoon Morakot events

Natural Hazards
and Earth System
Sciences
Discussions

1   In this period, the amount of total landslide area Aiyuzih subwatershed increased significantly

2   after the 1999 Chi-Chi Earthquake about 32 ha. And, the landslide distribution of Aiyuzih

3   subwatershed in this period ranged from 32.276 to 57.693 ha and its corresponding *LR* is

4   8.056% to 14.4%. And, the new landslide area caused by each event ranged from 3.027 to

5   24.528 ha and its corresponding *NLR* is 0.756% to 6.122%. In this period, most landslide area

6   occurred at the river source which of this mass of sediment creates a direct supply of sediment

7   material to the river and soon caused debris flows induced by 2004 typhoon Mindulle and

8   2008 typhoon Kalmaegi subsequently. Comparing this period with the previous period, the

9   total landslide area and new landslide area after 1999 Chi-Chi earthquake increased by 3.28

10   times and 2.4 times approximately. Again, the 1999 Chi-Chi earthquake also plays a key

11   component in landslide activity affecting all of rainfall event-triggered landslide distribution

12   including its number and magnitude in Aiyuzih subwatershed (see Fig.11).

13   c.   post-typhoon Morakot events

14   In this period, several large-scale landslide occurred after 2009 typhoon Morakot, most were

15   concentrated on the right river flank of the upstream watershed and oriented-north. The 2009

16   typhoon Morakot caused the new landslide area to increase to 86.590ha (*NLR*=21.613%) and

17   the total landslide area totals 133.036ha (*LR*=34.097%) which is more than a third of Aiyuzih

18   subwatershed area and it is indeed a greatest increase in total landslide area within its disaster

19   history as well as Chushui subwatershed.

20   **4.2   Spatial Landslide Distribution**

21   Landslides are generally a natural accompaniment of the geological cycles of uplift,

22   weathering and erosion. These long-term preparatory factors for landslides and the more local,

23   much shorter-term effects would trigger a particular failure (Hutchinson, 1995). To evaluate

24   all of the rainfall-induced landslide distribution in spatial scale for Chushui and Aiyuzih

25   subwatersheds, this study superimposed insights on geomorphology, geology, hydrology, and

26   human activity with regard to environmental and triggered factors. Accordingly, each unique

27   condition units (UCU) of landslide contribution (*LC*) was calculated to represent which

28   factors occupied most landslide distribution spatial scale and most possibly encourage future

29   landslide occurrence.

Natural Hazards
and Earth System
Sciences

Discussions

1　**(1) Geomorphology：elevation, slope and aspect**

2　A geomorphological map is used to depict elevation, slope gradient and aspect generated by

3　Digital Elevation Models (DEM) through a raster (grid) dataset of elevations. The elevation of

4　a mountain usually refers to its summit or divide which reflects climatic characteristics such

5　as temperature change and rainfall distribution. Landslides tend to occur on steeper slopes,

6　especially where the slope is covered by a thin colluvium. Aspect can influence moisture

7　retention and vegetation or drainage direction, which in turn can affect soil strength and

8　susceptibility to landslide (Chang *et al.*, 2007). So, this study use high-precision 5mx5m

9　DEM of the Shenmu watershed (see Fig.12) to derive geomorphology maps of elevation,

10　slope (in degrees) and aspect (see Fig.13~14) to assess landslide distribution in spatial scale

11　for each event. Figure 13 represents elevation of Chushui and Aiyuzih subwatersheds ranged

12　from 1000-3000m and 1000m-2500m. Both of the two elevation maps are divided into six

13　intervals by 500m spacing units for statistics of landslide distribution change affected by the

14　Chi-Chi earthquake. The results show landslide contribution (*LC*) of Chushui subwatersheds

15　subjected to 1996 typhoon Herb and 1999/5/28 heavy rainfall before Chi-Chi earthquake

16　concentrated in the interval of 2000-2500m elevation, which ranged from 42.51 to 54.16%

17　and averaged approximately 49.27%. After the Chi-Chi earthquake, the landslide contribution

18　(*LC*) affected by extreme rainfall events has dropped to 29.03%. Highest landslide

19　contribution (*LC*) belonged to the interval of 1500-2000m which ranged between 43.60 to

20　63.19% and averaged 52.38% with an increase by 1.21 times compared with the value before

21　the Chi-Chi earthquake. After 2009 typhoon Morakot, the highest landslide contribution still

22　belongs to the interval of 1500-2000m elevation about 53.08%. Consequently, it can be

23　deduced that typhoon-induced landslide potential in Chushui subwatersheds have gradually

24　moved towards the downstream watershed area with time obviously after 1999 Chi-Chi

25　earthquake. On the other hand, landslide contribution (*LC*) of Aiyuzih subwatersheds mainly

26　belonged to the interval of 1500-2000m which averaged close to 58% whether before and

27　after the Chi-Chi earthquake. (see Fig.15~16).

28　In terms of slope, according to Taiwan technical regulations for soil and water conservation

29　(SWCB, 2006), slopes are divided into seven classes (see Table 3). In consideration to the

30　environmental factor of slope, landslide contribution (*LC*) of Chushui and Aiyuzih

31　subwatersheds was mainly concentrated in class VI and VII sloppes before and after the Chi-

Natural Hazards
and Earth System
Sciences
Discussions

EGU
Open Access

1　Chi earthquake. After typhoon Morakot, the average of two subwatersheds was between 65.58

2　to 83.31%. In addition, in consideration to the environmental factor of aspect, landslide

3　contribution (*LC*) of Chushui and Aiyuzih subwatersheds was mainly concentrated on west-

4　facing and southeast-facing slopes before and after the 1999 Chi-Chi Earthquake (see Fig.

5　15~16).

6　Namely, seismic effect did not affect the slope or aspect of geomorphological factor evidently,

7　but elevation under seismic effect has more dominated landslide distribution than the other

8　geormorphological factors in these watersheds.

9　**(2) Geology：Lithology**

10　Landslide occurrence influenced by geological factor is determined by the lithological

11　characteristics, formation and degree of weathering. If the geological formation is fractured,

12　high-permeability, exhibiting shallow soil layers and dense faults, this may influence severe

13　and frequent landslides in subsequent heavy rainfall events (Chen *et al*., 2014). Except the

14　few downstream alluvial places, most geological setting of Chushui subwatershed is

15　Nanchuang Formation. Therefore, most typhoon/rainfall-triggered landslides areas are located

16　within Nanchuang Formation. The average landslide contribution (*LC*) reaches 99% before

17　and after the 1999 Chi-Chi Earthquake (see Fig. 15~16). In contrast, the geological setting of

18　Aiyuzih subwatershed is composed of Nanchuang Formation in upstream area and Hoshe

19　Formation in downstream area. The average landslide contribution (*LC*) of Nanchuang

20　Formation ranged between 71.66 to 82.19% and is greater over Hoshe Formation before and

21　after the 1999 Chi-Chi Earthquake (see Fig. 15~16).

22　Lin *et al*. (2008) has studied on typhoons and earthquakes on rainfall-induced landslides in

23　central Taiwan and also found that landslide distribution is intimately related with the uniaxial

24　compressive strength. They concluded that the average uniaxial compressive strength of

25　Nanchuang Formation, at 42 MPa, is lower than the average uniaxial compressive strength of

26　Hoshe Formation and the increase in the landslide ratio of Nanchuang Formation is higher

27　than the increase of Hoshe Formation which also agree well with the above observations.

28　**(3) Hydrology：river erosion and rainfall**

29　The influence of river erosion on the landslide phenomena activation is expressed in the

30　transportation of the sediment material from lower retaining parts of the slopes and

1   disturbance to the slope equilibrium. The lateral erosion (toe-cutting) is observed mainly in

2   rivers with constant water current. The activity of the rivers bearing their own sediments,

3   when changes in the water level occur, easily leads to rapid alternations in the position of

4   riverbeds or the offset of river course (Margottini *et al*., 2013). Consequemtly, it would

5   positively encourage the activation of landslide process especially when suffering exreme

6   rainfall events. For evaluating landslide correlated with river erosion, a buffer zone was set to

7   external expansion 25m on both sides of the river system for statistical analysis of landslide

8   contribution (*LC*) of Chushui and Aiyuzih subwatersheds (SWCB, 2010[a]). Figure 15~16

9   shows most typhoon/rainfall-triggered landslides areas of the two subwatersheds are located

10 within a buffer zone of river system before and after the 1999 Chi-Chi Earthquake. After the

11 1999 Chi-Chi Earthquake, landslide contribution of both watersheds affected by river erosion

12 is significantly increasing year upon year and has reached the peak after the 2009 typhoon

13 Morakot. Landslides is discernibly identified along river courses with the two watersheds

14 especially in the past ten years.

15 On the other hand, the modified Uchihugi formula based on Eq. (4) can be employed to depict

16 the relationship between the new landslide ratio of each event versus its corresponding

17 accumulated rainfall. Figure 17 represents accumulated rainfall increases which would indeed

18 enlarge the new landslide ratio of the two subwatersheds. It is obvious that the corresponding

19 accumulated rainfall is a major triggering factor to induce landslide occurrence during

20 typhoon season. It could be inferred that the new landslide ratio of Aiyuzih subwatershed is

21 averagely greater than Chushui subwatershed over 1.64 times subjected to the same

22 accumulated rainfall of pseudo event.

23 **(4) Human activity：land use and road construction**

24 Human activities with regard to land use such as the planting of crops, clearance of vegetation

25 or geotechnical engineering projects such as road construction have important effects on slope

26 instability (Cotecchia, 1978; Greenway 1987; Hutchinson, 1995). It is indicated that land use

27 belonging to bare land such as streams, canals and shoal of Chushui and Aiyuzih

28 subwatersheds have landslide contribution (*LC*) greater than 56% at least before and after the

29 1999 Chi-Chi Earthquake (see Fig. 15~16). Also, these observations are fitted with the results

30 from the influence of river erosion on the landslide which infers majority of typhoon/rainfall-

31 triggerred landsides are activated or reactivate close to the river courses.

Natural Hazards
and Earth System
Sciences

Open Access

EGU

Discussions

1   Similarly to evaluate landslide correlation with road construction, a buffer zone was set to

2   external expansion of 25m on both sides of the road network for statistical analysis of

3   landslide distribution of Chushui and Aiyuzih subwatersheds (SWCB, 2010[a]). Since no road

4   passes through Aiyuzih subwatershed, the landslide contribution is zero. Moreover, Highway

5   18 has passed through the south of Chushui subwatershed and the average landslide

6   contribution only reaches from 3.76~4.85% with a buffer zone of road network. It is evident

7   that there is less relevant correlation with human activity. (see Fig. 15~16)

8   **5.   Discussion**

9   **5.1   Earthquake Amplification Effect**

10 Sediment-related disasters, including debris flow and landslides, have frequently occurred in

11 Taiwan during the past two decades, especially following the 1999 Chi-Chi earthquake ($M_L =$

12 7.3). The most well-documented recent debris-flow events were those caused by typhoons,

13 including 2001 typhoon Toraji, 2004 typhoon Mindulle and 2009 typhoon Morakot (Cheng et

14 al., 2005; Chang *et al*., 2007; Tsai et al., 2010; Wu et al., 2011; Lo et al., 2012; Chen, et al.,

15 2014). The Shenmu watershed was approximately 36 km from the epicentre of the 1999 Chi-

16 Chi earthquake, during which the peak ground acceleration (PGA) reached betwwen 250 to

17 400 gal (Chung, 1999). As the previously mentioned, spatial and statistical results based on

18 the complete landside inventory maps of both Chushui and Aiyuzih subwatersheds exhibited

19 that in temporal-scale distribution, the three major sediment-related disasters highlights a

20 significant increase of landslide ratio. Until October, 2009 after typhoon Parma, the statistics

21 shows the total landslide areas of Aiyuzih subwatershed was about 2 times more than Chushui

22 subwatersheds. That proves the strong seismic effect of 1999 Chi-Chi earthquake has

23 destructive impact on local geological condition due to the lithological strength and structure,

24 which can lead to the weakening of the cohesion and strength of rock and soil mass near

25 hillcrests, which in turn can lead to more or large-scale typhoon/heavy rainfall-triggered

26 future landslides occurrence after an earthquake (Havenith *et al*., 2006, Chang *et al*, 2007).

27 From a geographical point of view, both of Chushui and Aiyuzih subwatersheds located at

28 Alishan mountain belong to one of the top five highest mountains in Taiwan. Also, Aiyuzih

29 subwatersheds is closer in the proximity of the Chi-Chi earthquake epicenter with smaller area

1 and steeper terrain than Chushui subwatersheds. Geli *et al.* (1988) has found that earthquake-

2 triggered landslides have been related to the topographic characteristics as well as

3 amplification effect of topography, which means seismic motion is amplified at mountain tops.

4 In addition, the proximity to the earthquake epicentre and earthquake fault has been suggested

5 by Keefer (2000) as proportional to the surface area disturbed by landsliding and the increase

6 becomes more obvious with proximity to the epicenter. The landslide data of Chi-Chi

7 earthquake was highlighted by Dadson *et al.* (2004) whose findings stated that the decrease in

8 area affected by landslide away from the Chelungpu fault was rapid at distances in excess of

9 20 km from the fault (see Fig.18). Accordingly, it can be logically deduced that Aiyuzih

10 subwatersheds after 1999 Chi-Chi earthquake, the landslide ratio increased more obviously

11 than Chushui subwatersheds with proximity to the epicentre especially subjected to 2009

12 typhoon Morakot.

13 **5.2 Combination of Causative Factors**

14 Through the obtained results from the previous spatial and statistical analysis with

15 environmental factors related to landslide inventory, a combination of causative factors for

16 any given area within the study area can be elaborated. Figure 19 represents the average

17 landslide contribution (*LC*) of various environmental/causative factors after 1999 Chi-Chi

18 earthquake for Chushui and Aiyuzih subwatersheds. These causative factors are also

19 subdivided into natural and anthropogenic factors. Among them, anthropogenic factors (as

20 well as human activity including land use and road construction) cause minor or irrelevant

21 landslide contribution in the two subwatersheds, but natural factors (including elevation, slope

22 gradient, lithology and river erosion) dominate landslide contribution within the study area.

23 This means these two areas have infrequent human interference and landslide process is only

24 controlled by typhoon/heavy rainfall events during flood season. Afterward, the combination

25 of major relevant causative factors would be arranged to set a series of logic reason-based rule

26 due to the studied results as shown in Fig. 20~22. The attributes of highest-potential landslide

27 location are concluded to be situated on 1500m ~2000m of elevation which of slope gradient

28 over 55% and oriented west/southeast, lies in Nanchuang Formation and adjacent to a 25m

29 buffer zone of river course. Furthermore, using logic reason-based rules can quickly detect or

Natural Hazards
and Earth System
Sciences

Open Access

EGU

Discussions

1   assess the future landslide locations and then can serve as the basis for effectively managing

2   watersheds, planning of disaster prevention works and reducing risk of landslide in advance.

3   **5.3   Landslide Potential Map**

4   The contribution and functional relationship between various factors (environmental and

5   triggering) affecting slope instability, the spatial-temporal distribution of landslides and the

6   prediction of landslide occurence has been highlighted in many studies throughout the past

7   century and has gained increased scrutiny from researchers in recent years (Guzzetti et al.,

8   1999; Ayalew and Yamagishi, 2005). This study utilized the logic reason-based rules based

9   on a combination of geomorphology, geology, hydrology and other environmental factors to

10   assess and delineate the future landslide potential area of the two watersheds. The generally

11   accepted correlation between past and future factors leading to slope instability or leading to

12   landslide occurence has been highlighted by previous researchers (Clerici et al., 2006). The

13   results revealed that areas which have well-vegetated land cover presently have no evidence

14   of landslide activity (ie. there are no signs of collapse or active areas). Based on the

15   assumption that impact of triggerring factors are excluded, landslide potential of the two

16   watersheds have been assessed, categorized, and mapped into three classes. These classes

17   constitute a clear and definite representation of the relative levels of future landslide

18   occurrence threat. The future landslide potential map of Chushui and Aiyuzih subwatersheds

19   are composed of three classes as follows: low, moderate and high. In practical applications,

20   the low potential landslide areas fit any one of the developed three logic reason-based rules

21   based on a combination of environmental factors as show in Fig. 20. Secondly, the moderate

22   potential landslide areas fit any two of the developed three logic reason-based rules based on a

23   combination of environmental factors as show in Fig. 21. Finally, the high potential landslide

24   areas fit all of the developed three logic reason-based rules based on a combination of

25   environmental factors as show in Fig. 22.

26   According to Fig. 23, the landslide potential map of Chushui and Aiyuzih subwatersheds are

27   regularly delineated and then generated qualitatively. Table 4 lists statistics of three classes

28   potential of landslide area within the two subwatersheds. The landslide potential area of

29   Chushui subwatersheds still exists about 721.11 ha which involved 112.3 ha of moderate and

30   high potential landslide area occupied in 13.24% of the whole watershed. And, the landslide

1 potential area of Aiyuzih subwatersheds still exists about 231.11 ha which involved 31.7 ha of

2 moderate and high potential landslide area occupied in 2.72% of the whole watershed.

3 Comparing both subwatersheds, high potential landslide area of Chushui subwatersheds is 3.3

4 ha more than Aiyuzih, and the largest part of areas are 1.53 ha located at right flank of the

5 middle river portion. In contrast, the high potential landslide area of the Aiyuzih subwatershed

6 have occurred mostly in past so that there only rests 0.1 ha of the high potential landslide area

7 located at the left flank of upstream subwatershed adjacent to river source.

8 From a risk assessment point of view, investigations of elements at risk in the two

9 subwatersheds conclude the native population who live, work and travel through the area

10 suffer and has limited number of properties such as houses and buildings are the greatest

11 exposed to landslide hazard. Landslide risk to these elements at risk is generally seen as low

12 within the two subwatersheds. However, some residents of Shenmu Village at present still

13 live close to the confluence of two subwatershed where Highway 21 passes through the

14 Shenmu Bridge and the Elementary School constructed nearby. Therefore, the instantaneous

15 evolution of moderate and high potential landslide area should be paid more attention to and

16 periodically monitored depending on remote sensing images (satellite/radar images and aerial

17 photos) or using the long-term observation stations equiped with rainfall gauges, geophones

18 and others especially during the typhoon season and then conduct rapid decision-making

19 process to set sophisticated engineering measures or implement rapid evacuation responses

20 for effectively reducing damages, loss of life and risk from the debris-flows disaster caused by

21 the potential landslide area under extreme rainfall condition.

6. Conclusion

23 Landslide and other sediment-related disasters are a natural phenomena related to the cycle of

24 land degradation which affects many populations world-wide. In Taiwan, landslides are

25 frequent occurences especially during extreme events such as earthquakes and typhoons.

26 Under the effect of global climate change, the probability of extreme weather occurrence has

27 increased. These events act as triggering factors for landslides on unstable slopes. Therefore,

28 landslide frequency in Taiwan has seen an increase over time. The cycle of land degradation

29 and the high uncertainty with recurrent characteristics of landslides has led to the formation of

30 vast amounts of unstable sediment material deposited on hillslopes which could easily lead to

Natural Hazards
and Earth System
Sciences

Open Access

EGU

Discussions

1   other secondary disasters (eg. landslide dams and debris flows). Furthermore, landslide

2   processes are a complicated mechanism which is further complicated by the various triggering

3   factors combined with causative factors (eg. environmental factors) depending on the local

4   characteristics of specific region or given watershed scale. Through spatial analysis of multi-

5   event landslide inventory maps, it can be deduced that the estimated/predicted potential

6   landslide area inherits a combinations of causative factors of the historical landslide

7   experienced in the watershed/slope. Then, the landside inventory maps from 1996 typhoon

8   Herb to 2009 typhoon Parma is established systematically and exhaustively by semi-

9   automated image interpretation and artificial image identification procedures for ensuring the

10   completeness and accuracy of the dataset composing 11 historical disaster event involving 17

11   satellite images set. This study used the proposed methods based on the developed event-

12   based landside inventory maps to analyze the overall landslide evolution, magnitude of

13   landslide, landslide location and landslide potiental affecting by these extreme events in time

14   and space domains. Also, the strong seismic effect of 1999 Chi-Chi earthquake and the

15   quantified magnification of this event on amount of landslide for subsequent typhoon events

16   were included in this study. Finally, the studied results and concrete observation can be

17   concluded as follows:

18   1. The study suggests a framework for semi-automated image interpretation and artificial

19   image identification procedures which dramatically improves the quality of data content

20   and data structure so that it can definitely promote data integrity and accuracy for

21   improving value and reliability of event-based landslide inventories. For ensuring data

22   integrity, it is necessary to utilize high-resolution satellite image set close to the date of

23   event occurrence and also cross check the collected historical aerial photographs and local

24   landslide reports in order to reduce the influence of artefacts which result in data

25   imperfection or deficiency of landslide inventory such as cloud cover after the disaster

26   event or shadowing which leads to omission of the interpreted landslide polygon subject.

27   For controlling data accuracy, image registration should first be conducted for all of the

28   satellite image in order to reduce spatial location shifting of image causing false positives.

29   In addition, the land use/land cover map and aerial photographs are used to eliminate

30   likely-landslide polygon due to human activities for extracting the real landslide area

31   caused by natural hazard. The above framework can be applied to similar research to

1 study the completeness of landslide inventory with enviromental factors for any given

2 area.

3 2. The results of temporal scale analysis of the landslide inventories are used to classify the

4 event which caused the highest increase in landslide area among the three designated

5 periods. Before the 1999 Chi-Chi earthquake, the extreme events with the greatest impact

6 on Chushui and Aiyuzih subwatersheds were regarded as 1996 typhoon Herb and

7 1999/5/28 heavy rainfall respectively. From 1999 Chi-Chi earthquake to pre-typhoon

8 Morakot, the extreme events with the greatest impact was 2004 typhoon Mindulle. In

9 view of the post-typhoon Morakot events, it is obvious that 2009 typhoon Morakot

10 resulted in the greatest impact on the two watersheds with a large increase in landslide

11 area. After comparisons were made of the total landslide and new landslide area before

12 and after 1999 Chi-Chi earthquake in the two subwatersheds, it was found that the

13 earthquake amplification effect of the quantified magnification was estimated to be at

14 least doubled that agrees well with the previous studies. Furthermore, from the

15 relationship between the new landslide ratio of each event versus its corresponding

16 accumulated rainfall, the modified Uchihugi formulas of two subwatersheds could be used

17 to quickly estimate new landslide area caused by of a given event during typhoon season

18 depending on the parameter of accumulated rainfall. Estimation of the new landslide area

19 caused by an event can provide useful information as a reference basis for preliminary

20 evaluation of the exposure of elements at risk downstream for early warning , rapid

21 response, urgent evacuation and longterm mitigation solutions.

22 1. According to the long-term average trend of landslide contribution after the Chi-Chi

23 earthquake events, it can represent which environmental factors are major relevent

24 causative factors and be further utilized to establish as a series of logic reason-based rules

25 to delineate potential landslide areas. Accordingly, the generated landslide potential map

26 based on the developed logic reason-based rules may be as simple as a semi-quantitative

27 map that can be used to display the locations of old and new landslides to indicate

28 potential instability. For moderate-high potential landslide area, it is recommended to

29 construct preventive engineering measures by its necessity and requirement of

30 remediation or utilize education for effectively reducing loss of life and damage to public

31 property and making landslide risks more tolerable and generally acceptable limit.

References

1. Aleotti, P., (2004), "A warning system for rainfall-induced shallow failures", Engineering Geology, Vol. 73, No. 3, pp. 247-265.

2. Aleotti, P., and Chowdhury, R. (1999), "Landslide hazard assessment: summary review and new perspectives", Bulletin of Engineering Geology and the Environment, Vol. 58, Issue 1, pp. 21-44.

3. Ayalew L., and Yamagishi, H. (2005), "The application of GIS-based logistic regression for landslide susceptibility mapping in the Kakuda-Yahiko Mountains, Central Japan", Geomorphology, Volume 65, Issues 1-2, pp. 15-31.

4. Bai, S. B., Wang, J., Lu, G. N., Zhou, P. G., Hou, S. S. and Xu S. N. (2009), "GIS-based and data-driven bivariate landslide-susceptibility mapping in the Three Gorges Area, China", Pedosphere, Vol. 19, Issue 1, pp 14-20.

5. Barlow, J., Franklin, S. and Martin, Y. (2006), "High spatial resolution satellite imagery, DEM derivatives, and image segmentation for the detection of mass wasting processes", Photogrammetric Engineering and Remote Sensing, Vol. 72, No. 6, pp 687-692.

6. Bonham-Carter, G. F. (1994), "Geographic information systems for geoscientists: modeling with GIS", New York, Pergamon/Elsevier Science Inc.

7. Borghuis, A. M., Chang, K. and Lee, H. Y. (2007), "Comparison between automated and manual mapping of typhoon-triggered landslides from SPOT-5 imagery", International Journal of Remote Sensing, Vol. 28, Issue 8, pp. 1843-1856.

8. Caine, N., (1980), "The rainfall intensity-duration control of shallow landslides and debris flows", Geografiskam Annaler, Vol. 62, pp. 23-27.

9. Carrara, A., Cardinali M., and Guzzetti, F., (1992), "Uncertainty in assessing landslide hazard and risk", ITC Journal, The Netherlands 2, pp 172-183.

10. Carrara, A., Cardinali, M., Guzzetti, F., and Reichenbach, P. (1995) "GIS technology in mapping landslide hazard", Geographical Information Systems In Assessing Natural Hazards, Kluwer, Dordrecht, pp 135-176.

11. Carrara, A., Guzzetti, F., Cardinali, M., and Reichenbach, P., (1999), "Use of GIS technology in the prediction and monitoring of landslide hazard", Natural hazards, Vol. 20, Issue 2, pp 117-135.

12. Castilla, G., Larkin, K., Linke, J. and Hay, G. J. (2009), "The impact of thematic

Natural Hazards
and Earth System
Sciences
Discussions

1   resolution on the patch-mosaic model of natural landscapes", Landscape Ecology, Vol. 24,
2   Issue. 1, pp. 15–23.

3   13. Chang, K. T., Chiang, S. H., Chen, Y. C., and Hsu, M. L. (2007), "Modeling typhoon- and
4   earthquake-induced landslides in a mountainous watershed using logistic regression",
5   Geomorphology, Vol. 89, Issues 3-4, pp. 335-347.

6   14. Chang, K. T., Chiang, S. H., Chen, Y. C., and Mondini, A. C. (2014), "Modeling the
7   spatial occurrence of shallow landslide triggered by typhoons", Geomorphology, Vol. 208,
8   pp. 137-148.

9   15. Chau, K. T. and Lo, K. H. (2004), "Hazard assessment of debris flows for Leung King
10   Estate of Hong Kong by incorporating GIS with numerical solutions", Natural Hazards
11   and Earth System Sciences., Vol. 4, pp 103-116.

12   16. Chen, S C., Chou, H. T., Chen, S. C., Wu, C. H., and Lin, B. S. (2014), "Characteristics of
13   rainfall-induced landslides in Miocene formations: a case study of the Shenmu watershed,
14   Central Taiwan," Engineering Geology, Vol. 169, pp. 133-146.

15   17. Chen, S. C., and Wu, C. H. (2006), "Slope stabilization and landslide size on Mt. 99 Peaks
16   after Chi-Chi Earthquake in Taiwan", Environmental Geology, Vol. 50, Issue 5, pp 623-
17   636.

18   18. Chen, W. F. and Cheng, H. H. (1997), "Application of remote sensing and GIS in
19   assessing changes of the large-scale land development of watershed", Journal of Soil and
20   Water Conservation, Vol. 29, No.1, pp. 41-59. (in Chinese)

21   19. Cheng, J. D., Huang, Y. C., Wu, H. L., Yeh, J. L., and Chang, C. H. (2005),
22   "Hydrometeorological and land use attributes of debris flows and debris floods during
23   typhoon Toraji, July 29－30, 2001 in central Taiwan", Journal of Hydrology, Vol. 306,
24   Issues 1-4, pp. 161–173.

25   20. Chung, C F., Fabbri, A. G., van Westen, C. J. (1995), "Multivariate regression analysis for
26   landslide hazard zonation", Geographical information systems in assessing natural hazards,
27   Kluwer, Dordrecht, pp 107-133

28   21. Chung, J. K. (1999) "Report on Chi-Chi Earthquake of September 21, 1999", Central
29   Weather Bureau, Taiwan.

30   22. Clerici, A., Perego, S., Tellini, C. and Vescovi, P. (2006), "A GIS-based automated
31   procedure for landslide susceptibility mapping by the Conditional Analysis method: the

Natural Hazards
and Earth System
Sciences
Discussions

Open Access

EGU

Baganza valley case study (Italian Northern Apennines)", Environmental Geology, Vol. 50, Issue 7, pp 941-961.

23. Coe, J. A., Michael, J. A., Crovelli, R. A., and Savage, W. Z. (2004), "Probabilistic assessment of precipitation-triggered landslides using historical records of landslide occurrence, Seattle, Washington", Environmental and Engineering Geosciences, Vol. 10, pp. 103-122.

24. Crozier, M. J., (1986), "Landslides: causes, consequences and environmental perceptions" Croom Helm, London.

25. Cruden, D. M., and Varnes D. J. (1996), "Landslide types and processes", Landslides: investigation and mitigation, Transportation research board special report 247, Washington, pp. 36-75.

26. Dadson, S. J., Hovius, N., Chen, H., Dade, W. B., Hsieh, M. L., Willett, S. D., Hu, J. C., Horng, M. J., Chen, M. C., Stark, C. P., Lague, D., and Lin, J. C., (2003), "Links between erosion, runoff variability and seismicity in the Taiwan orogen", Nature, Vol. 426, pp. 648-651.

27. Dadson, S. J., Hovius, N., Chen, H., Dade, W. B., Lin, J. C., Hsu, M. L., Lin, C. W., Horng, M. J., Chen, T. C., Milliman, J., and Stark, C. P. (2004), "Earthquake triggered increase in sediment delivery from an active mountain belt", Geology, Vol. 32, No. 8, pp. 733-736.

28. Desclée, B., Bogaert, P., and P. Defourny, (2006), "Forest change detection by statistical object-based method", Remote Sensing of Environment, Vol. 102, Issues 1–2, pp. 1-11.

29. Fell, R., Corominas, J., Bonnard, Ch., Cascini, L., Leroi, E., and Savage, W.Z. (2008), "Guidelines for landslide susceptibility, hazard and risk zoning for land use planning", Engineering Geology, Vol. 102, pp. 99-111.

30. Geli, L., Bard, P. Y., and Jullien, B. (1988), "The effect of topography on earthquake ground motion: a review and new results", Bulletin of the Seismological Society of America February, Vol. 78, No. 1, pp. 42-63.

31. Glade, T., (2003), "Landslide occurrence as a response to land use change: a review of evidence from New Zealand", CATENA, Vol. 51, Issues 3-4, pp. 297-314.

32. Greenway, D. R. (1987), "Vegetation and slope stability", Slope Stability, John Wiley & Sons, pp. 187-230.

33. Guzzetti, F., Carrara A, Cardinali, M, and Reichenbach, P. (1999), "Landslide hazard

Natural Hazards
and Earth System
Sciences

Open Access

Discussions

EGU

1   evaluation: a review of current techniques and their application in a multiscale study,

2   Central Italy", Geomorphology, Vol. 31, Issues 1-4, pp. 181-216.

3 34. Havenith, H., Strom, A., Caceres, F., and Pirard, E. (2006), "Analysis of landslide

4   susceptibility in the Suusamyr region, Tien Shan: statistical and geotechnical approach.

5   Landslides, Vol. 3, Issue 1, pp 39-50.

6 35. Ho, H. C., Lin, B. S., Chi S. Y., Shih M. C. and Chen C. Y. (2011), "A Preliminary

7   investigation on the debris flow factors in Shenmu Area," Journal of Sinotech

8   Engineering, Vol. 110, pp. 41-51. (in Chinese).

9 36. Hutchinson, J. N. (1995), "Landslide hazard assessment", Landslides, Balkema,

10   Rotterdam, pp. 1805-1841.

11 37. Jakob, M, and Weatherly, H. (2003), "A hydroclimatic threshold for landslide initiation on

12   the North Shore Mountains of Vancouver, British Columbia", Geomorphology, Vol. 54,

13   Issues 3-4, pp. 137-156.

14 38. Joyce, K. E., Dellow, G. D., and Glassey, P. J. (2008) "Assessing image processing

15   techniques for mapping landslides", IEEE International Geoscience and Remote Sensing

16   Symposium, USA, pp. 1231-1234.

17 39. Kääb, A. (2002), "Monitoring high-mountain terrain deformation from repeated air- and

18   spaceborne optical data: examples using digital aerial imagery and ASTER data", ISPRS

19   Journal of Photogrammetry and Remote Sensing, Vol. 57, pp 39-52.

20 40. Keefer, D. K. (2000), "Statistical analysis of an earthquake-induced landslide distribution

21   - the 1989 Loma Prieta, California event", Engineering Geology, Vol. 58, Issues 3-4, pp.

22   231-249.

23 41. Lambin, E. F. and Strahlers, A. H. (1994), "Change-vector analysis in multitemporal

24   space: A tool to detect and categorize land-cover change processes using high temporal-

25   resolution satellite data", Remote Sensing of Environment, Vol. 48, Issue 2, pp. 231-244.

26 42. Lin, G. W., Chen, H., Chen, Y. H. and Horng, M. J. (2008), "Influence of typhoons and

27   earthquakes on rainfall-induced landslides and suspended sediments discharge",

28   Engineering Geology, Vol. 97, Issues 1-2, pp. 32-41.

29 43. Lo, W. C., Lin, B. S., Ho, H. C., Jeff Keck, Yin, H. Y. and Shan H. Y. (2012) "A Simple

30   and feasible process for using multi-stage high-precision DTMs, field surveys and rainfall

31   data to study debris-flow occurrence factors of Shenmu area, Taiwan," Special Issue:

Natural Hazards
and Earth System
Sciences

Discussions

Open Access

EGU

Documentation and Monitoring of Landslides and Debris Flows for Mathematical Modeling and Design of Mitigation Measures, Natural Hazards and Earth System Sciences, Vol. 12, pp. 3407-3419.

44. Lu, P., Stumpf, A., Kerle, N., and Casagli, N. (2011) "Object-oriented change detection for landslide rapid mapping", Geoscience and Remote Sensing Letters, IEEE, Vol. 8, Issue 4, pp. 701-705.

45. Malamud, B. D., Turcotte, D.L., Guzzetti, F., and Reichenbach P. (2004), "Landslide inventories and their statistical properties", Earth Surface Processes and Landforms, Vol. 29, Issues 6, pp. 687-711

46. Margottini, C., Canuti, P., and Sassa, K. (2013) "Social and economic impact and policies" Landslide Science and Practice, Vol. 7, Berlin, Springer, pp. 187-188.

47. Martha, T. R., Kerle, N., Jetten, V., van Westen, C. J., and Kumar, K. V. (2010), "Characterising spectral, spatial and morphometric properties of landslides for semi-automatic detection using object-oriented methods", Geomorphology, Vol. 116, pp. 24-36.

48. Mehrnoosh, J., Helmi, Z. M., Shafri, Mansor, S. B., Mohammad, S., S. Pirasteh (2009), "Landslide susceptibility evaluation and factor effect analysis using probabilistic-frequency ratio model", European Journal of Scientific Research, Vol. 33 Issue 4, pp 654.

49. Metternicht G., Hurni L., and Gogu R. (2005), "Remote sensing of landslides: An analysis of the potential contribution to geo-spatial systems for hazard assessment in mountainous environments", Remote Sensing of Environment, Vol. 98, pp 284-303.

50. Montgomery, D. R. and Dietrich, W. E. (1994), "A physically based model for the topographic control on shallow landsliding", Water Resources Research, Vol. 30, Issue 4, pp 1153-1171.

51. National Science and Technology Center for Disaster Reduction (2004), "Report on the analysis of sediment disaster problem at Shihmen reservoir, Xin-dian District, Taipei . (in Chinese)

52. Nichol, J., and Wong, M. S., (2005), "Satellite remote sensing for detailed landslide inventories using change detection and image fusion', International Journal of Remote Sensing, Vol. 26, Issue 9, pp. 1913-1926.

53. Soil and Water Conservation Bureau (2010a), "Field Investigation of Mechanism and Potential Analysis for Sediment Disaster in Shenmu Village, Shinyi Town, Nantou

1   County". (in Chinese)

2   54. Soil and Water Conservation Bureau (2010b), "Study on Historical Migration and Its

3   Mechanism of Heavy Rainfall-Induced Sediment Disaster in Shih-Men Watershed". (in

4   Chinese).

5   55. Soil Water Conservation Bureau (SWCB) (2006). "Technical Regulations for Soil and

6   Water Conservation" (in Chinese)

7   56. Trimble (2010) "Trimble Acquires Definiens' Earth Sciences Business to Expand Its

8   GeoSpatial Portfolio".

9   57. Tsai, F., Hwang, J. H., Chen, L. C. and Lin T. H. (2010), "Post-disaster assessment of

10   landslides in southern Taiwan after 2009 Typhoon Morakot using remote sensing and

11   spatial analysis", Natural Hazards and Earth System Science, Vol. 10, Issue 10, pp. 2179-

12   2190.

13   58. Uchiogi, T. (1971), "Landslides due to one continual rainfall." JSECE, Vol. 23, pp. 21-34

14   (in Japanese).

15   59. Van Westen, C. J. (2000), "Remote Sensing for natural disaster management",

16   International Archives of Photogrammetry and Remote Sensing. Vol. XXXIII, Part B7,

17   Amsterdam, The Netherlands, pp. 1609-1617.

18   60. Van Westen, C. J., Castellanos, E. and Kuriakose, S. L. (2008) "Spatial data for landslide

19   susceptibility, hazard, and vulnerability assessment: an overview", Engineering Geology,

20   Vol. 102, No.3, pp. 112-131.

21   61. Wu, C. H., Chen, S. C., and Chou, H. T. (2011), "Geomorphologic characteristics of

22   catastrophic landslides during typhoon Morakot in the Kaoping Watershed, Taiwan",

23   Engineering Geology, Vol. 123, Issues 1-2, pp. 13-21.

24   62. Yamaguchi, Y., Tanaka, S., Odajima, T., Kamai, T., and Tsuchida S. (2003), "Detection

25   of a landslide movement as geometric misregistration in image matching of SPOT HRV

26   data of two different dates", International Journal of Remote Sensing, Vol. 24, Issue 18,

27   pp. 3523-3534.

28

29

1

2   Table 1. Historical rainfall events and its corresponding rainfall data

Date	Rainfall event	R_A (mm)		Maximum rainfall intensity (mm/h)		Duration (hr)		Debris flow occurrence
		C	A	C	A	C	A	
1996/07/29 – 08/01	Herb	879	1987	70	112.5	96	173	C
1999/5/27-5/28	528 Heavy rainfall	284	313.5	21.5	23.5	48	24.5	C
2001/07/28 – 31	Toraji	587	757	75.5	121	96	82.5	C
2004/06/28 – 07/03	Mindulle	816.5	1181.5	45	84.5	144	10	A,C
2008/07/16 – 07/18	Kalmaegi	529.5	619	61.5	80	72	55	A,C
2008/07/26 – 07/29	Fung-wong	500	641.9	35	50	96	48	-
2008/09/11 – 09/16	Sinlaku	922	1470.5	30.5	53	144	83	-
2008/09/26 – 09/29	Jangmi	648	885.5	39.5	64.5	96	75.5	-
2009/08/05 – 08/10	Morakot	2099.5	3060.5	72	123	144	28.5	A,C
2009/10/03 – 10/06	Parma	18	154	3.5	31.5	96	19	-

3   Note 1: The A and C are referred to be Aiyuzi and Chushui subwatershed, respectively.
4   Note 2: R_A means accumulated rainfall of a given event.

5

6   Table 2. Correspondence between Historical Hazard Events and Satellite Images

NO.	Rainfall event (Date)	Satellite image sets			
		Stage	Date	Sensor	Resolution
1	Herb (1996/07/29–08/01)	pre-typhoon Herb	1996/04/17	SPOT-3	6.25 m
		post-typhoon Herb	1996/11/08	SPOT-2	6.25 m
2	528 Heavy rainfall (1999/5/27-5/28)	pre-528 heavy rainfall	1999/03/26	SPOT-4	6.25 m
		post-528 heavy rainfall	1999/07/24	SPOT-2	6.25 m
3	Chi-Chi Earthquake (1999/09/21)	post-earthquake Chi-Chi	1999/10/31	SPOT-4	6.25 m
4	Toraji (2001/07/28–31)	pre-typhoon Toraji	2001/01/20	SPOT-4	10 m
		post-typhoon Toraji	2001/10/22	SPOT-4	10 m
5	Mindulle (2004/06/28–07/03)	pre-typhoon Mindulle	2004/02/10	SPOT-5	2.5 m
		post-typhoon Mindulle	2004/07/10	SPOT-5	2.5 m
6	Kalmaegi (2008/07/16–07/18)	pre-typhoon Kalmaegi	2008/07/05	SPOT-5	2.5 m
		post-typhoon Kalmaegi	2008/07/21	SPOT-5	2.5 m
7	Fung-wong (2008/07/26–07/29)	post-typhoon Fung-wong	2008/08/26	SPOT-5	2.5 m
8	Sinlaku (2008/09/11–09/16)	post-typhoon Sinlaku	2008/09/21	SPOT-5	2.5 m
9	Jangmi (2008/09/26–09/29)	post-typhoon Jangmi	2008/11/12	SPOT-5	2.5 m
10	Morakot (2009/08/05–08/10)	pre-typhoon Morakot	2009/05/08	SPOT-5	2.5 m
		post-typhoon Morakot	2009/09/04	SPOT-5	2.5 m
11	Parma (2009/10/03–10/06)	post-typhoon Parma	2009/10/21	SPOT-5	2.5 m

7

8

1   Table 3. Landslide Correlation Hazard-Inducing Factor Classification in Chushui and Aiyuzih

2   subwatersheds

environmental category	Factor	Classification	
Geomorphology	Elevation (m)	0≤ elevation <500 500≤ elevation <1000 1000≤ elevation <1500	1500≤ elevation <2000 2000≤ elevation <2500 2500≤ elevation <3000
	Slope Gradient(%)	Class I: 0≤ slope <5% Class II: 5%≤ slope <15% Class III: 15%≤ slope <30% Class IV: 30%≤ slope <40%	Class V: 40%≤ slope <55% Class VI: 55%≤ slope <100% Class VII: ≥100%
	Slope Aspect(°)	North(N) Northeast(NE) East(E) Southeast(SE) South(S)	Southwest(SW) West(W) Northwest(NW) Flat
Geology	Lithology	Hoshe Formation	Nanchuang Formation
Hydrology	River Erosion	Set 25*m from the line to be the affected extent to compile landslide area within and not within this limit.	
	Rainfall	Typhoon Herb 528 heavy rainfall typhoon Toraji typhoon Mindulle typhoon Kalmaegi	typhoon Fung-wong typhoon Sinlaku typhoon Jangmi typhoon Morakot typhoon Parma
Human Activity	Land Use	Artificlal Forest Land Bared Land Cropland and Pasture Herbaceous Rangeland Nature Forest Land	Residential School Shrub and Brush Rangeland Streams and Canals Transportation
	road construction	Set 25*m from the line to be the affected extent to compile landslide area within and not within this limit.	

3   Note: slope classification system referred to SWCB (2006)

4

5   Table 4. statitics of low, moderate and landslide potential aread within Chushui and Aiyuzih

6   subwatersheds

Subwatershed area (ha)		Low potential landslide		Moderate potential landslide		High potential landslide		Total	
		Area (ha)	Occupied rate (%)	Area (ha)	Occupied rate (%)	Area (ha)	Occupied rate (%)	Area (ha)	Occupied rate (%)
Chushui	848.24	609.6	71.86%	109.0	12.85%	3.3	0.39%	721.9	85.1%
Aiyuzi	397.51	220.3	55.41%	10.7	2.70%	0.1	0.02	231.1	58.13%

7   Note: Ocupied rate (%) = (potential landslide area) / (subwatershed area)

8

Natural Hazards
and Earth System
Sciences

Discussions

Open Access
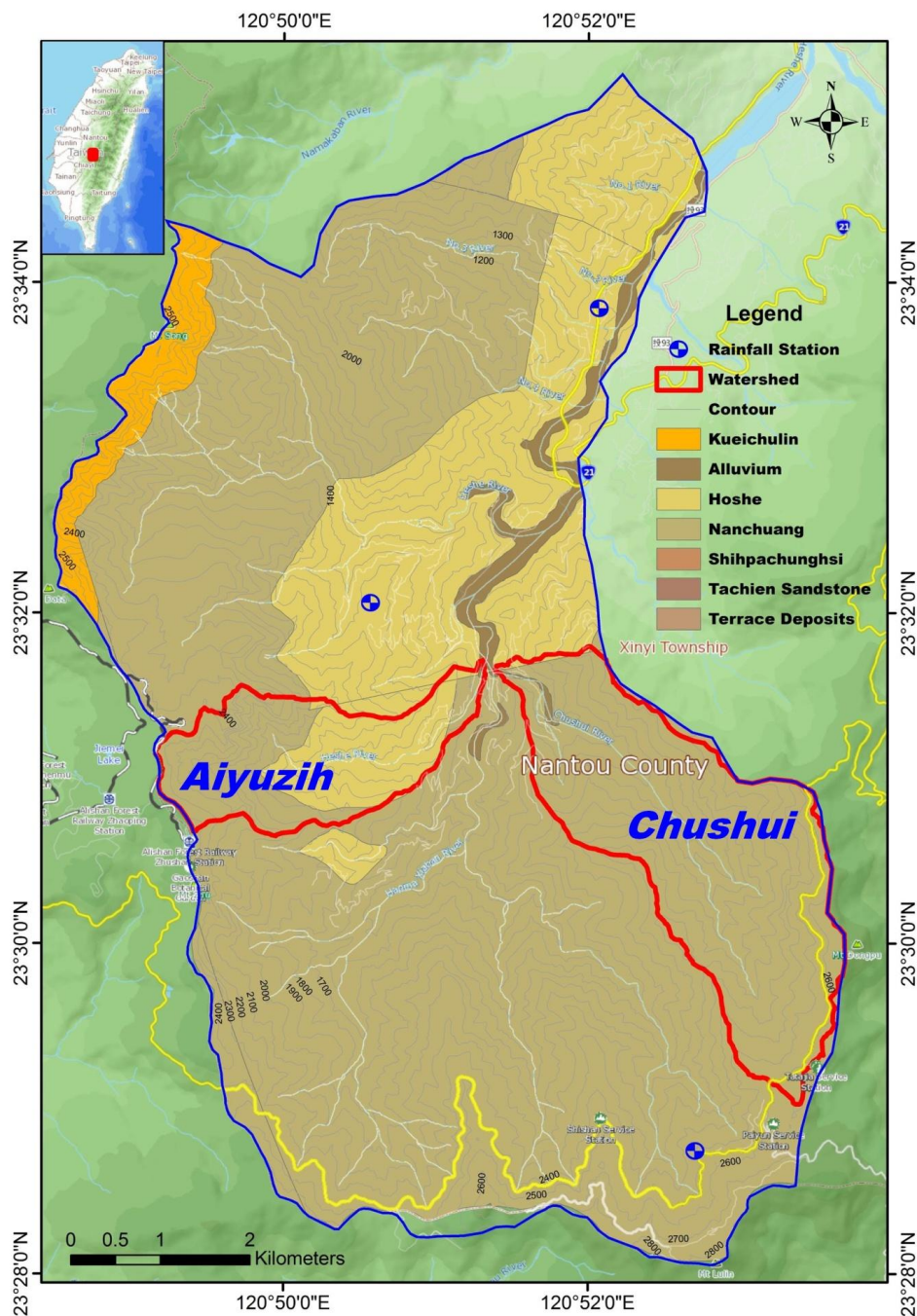
1

2   Figure 1. Geographic Location and Geology map of Shenmu area
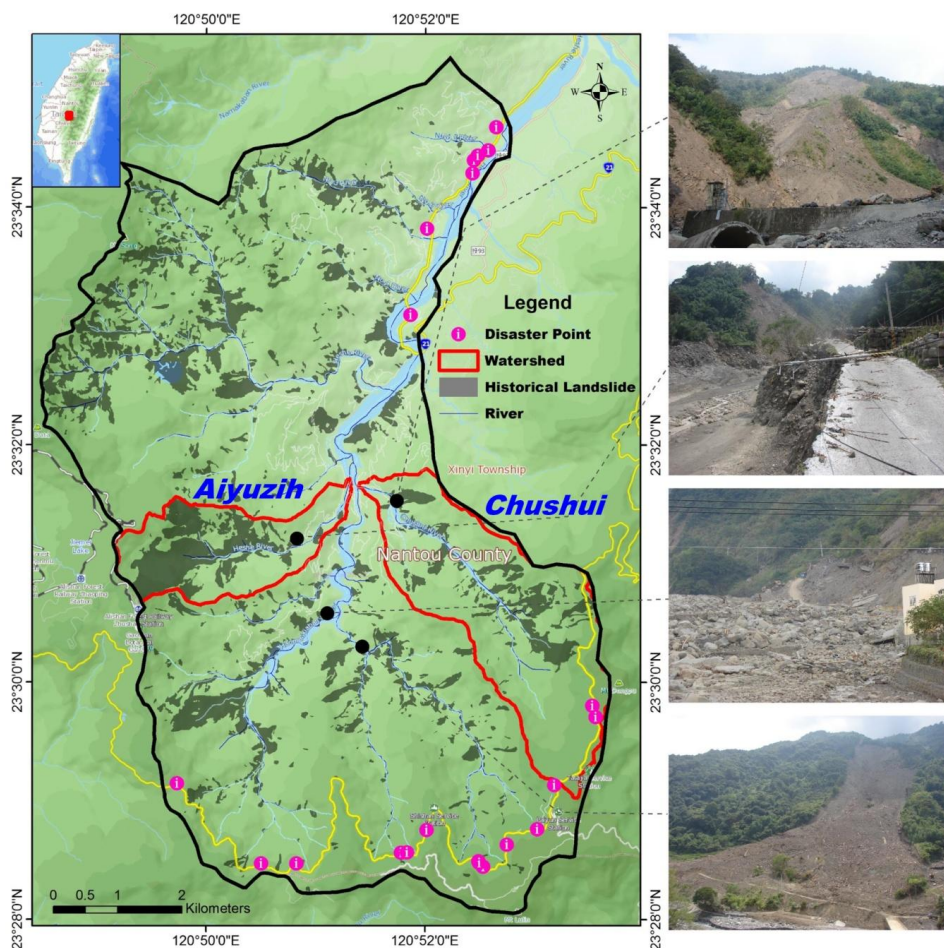
1

2   Figure 2 Landslide distribution and disaster points in Shenmu watershed after typhoon

3   Morakot

4
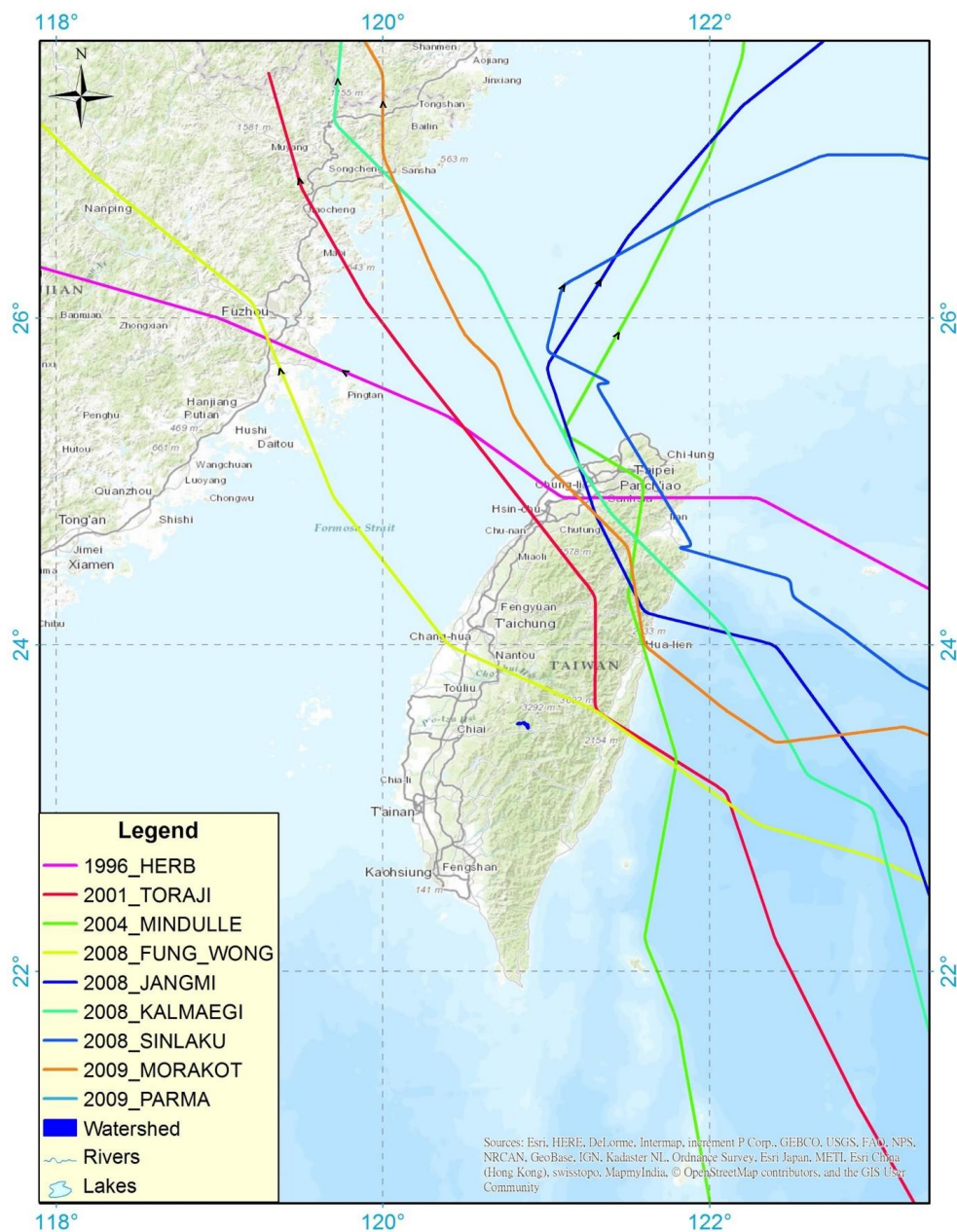
Figure 3. Path of Historical Typhoons which affected Taiwan.

Natural Hazards
and Earth System
Sciences
Open Access
Discussions

EGU

pre-typhoon
Herb(1996/04/17)

post-typhoon
Herb(1996/11/08)

pre-528 heavy
rainfall(1999/03/26)

post-528 heavy
rainfall(1999/07/24)

post-earthquake Chi-
Chi(1999/10/31)

pre-typhoon
Toraji(2001/01/20)

post-typhoon
Toraji(2001/10/22)

pre-typhoon
Mindulle(2004/02/10)

post-typhoon
Mindulle(2004/07/10)

pre-typhoon
Kalmaegi(2008/07/05)

post-typhoon
Kalmaegi(2008/07/21)

post-typhoon Fung-
wong(2008/08/26)

post-typhoon
Sinlaku(2008/09/21)

post-typhoon
Jangmi(2008/11/12)

pre-typhoon
Morakot(2009/05/08)

post-typhoon
Morakot(2009/09/04)

post-typhoon
Parma(2009/10/21)

1   Figure 4. Schematic layout of the adopted satellite images set

Natural Hazards
and Earth System
Sciences

Discussions

1
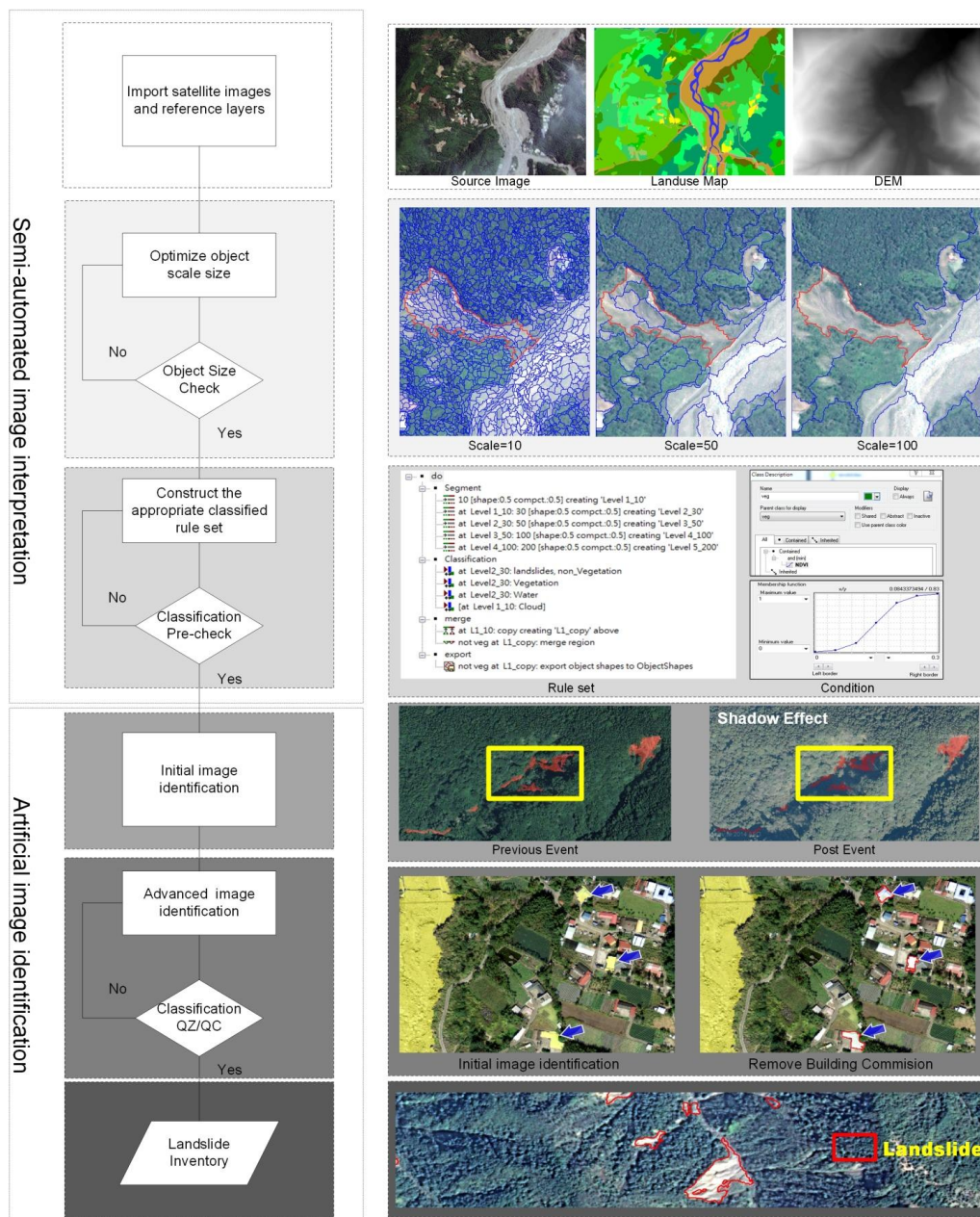
2
3   Figure 5. Procedure of the proposed image interpretation and identification
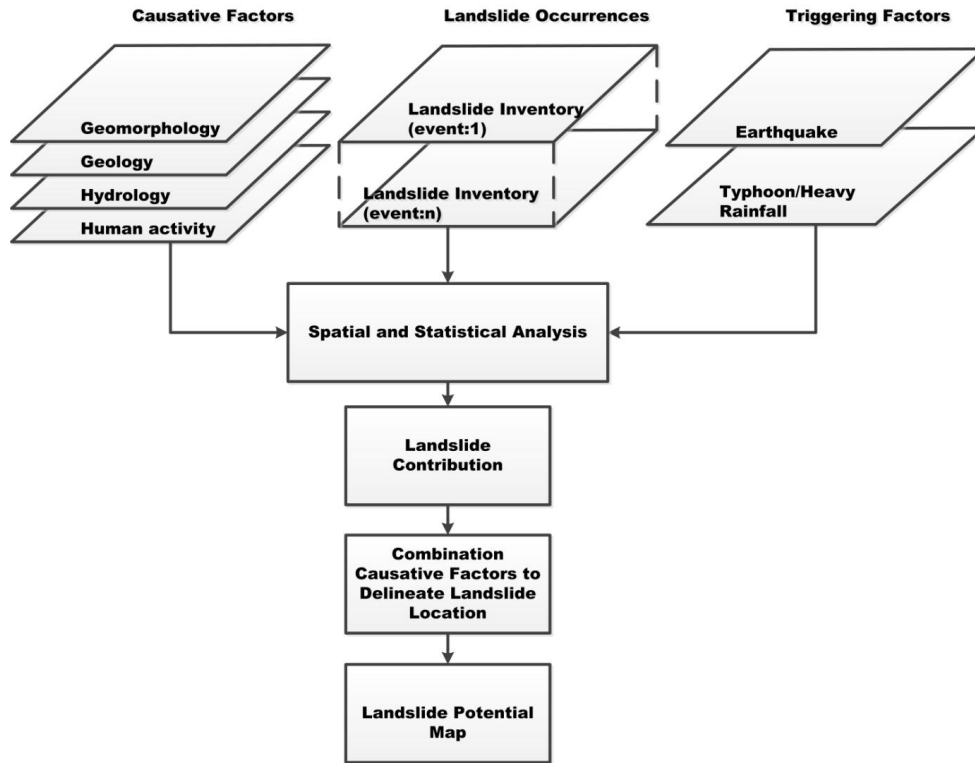
1

2   Figure 6. Procedure of spatial and statistical analysis environmental and triggered factors with

3   landslide inventory maps

4
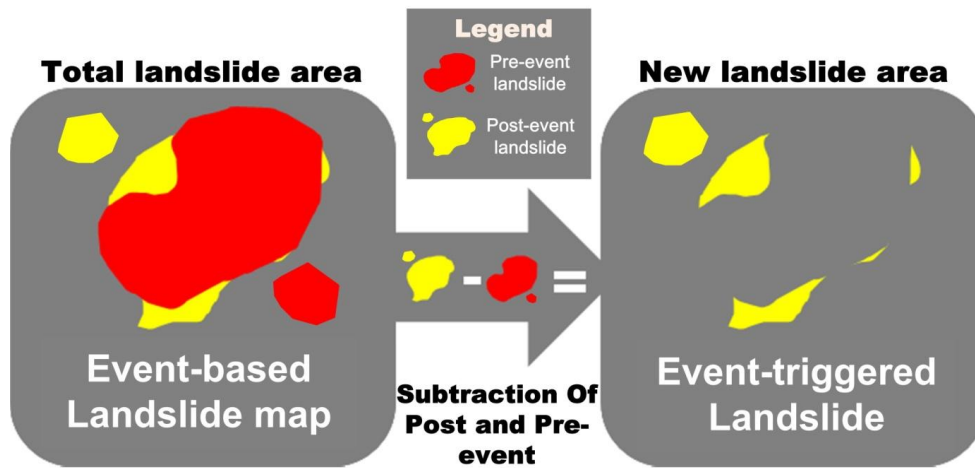
5

6   Figure 7. Sketch of total and new landslides area definition

1
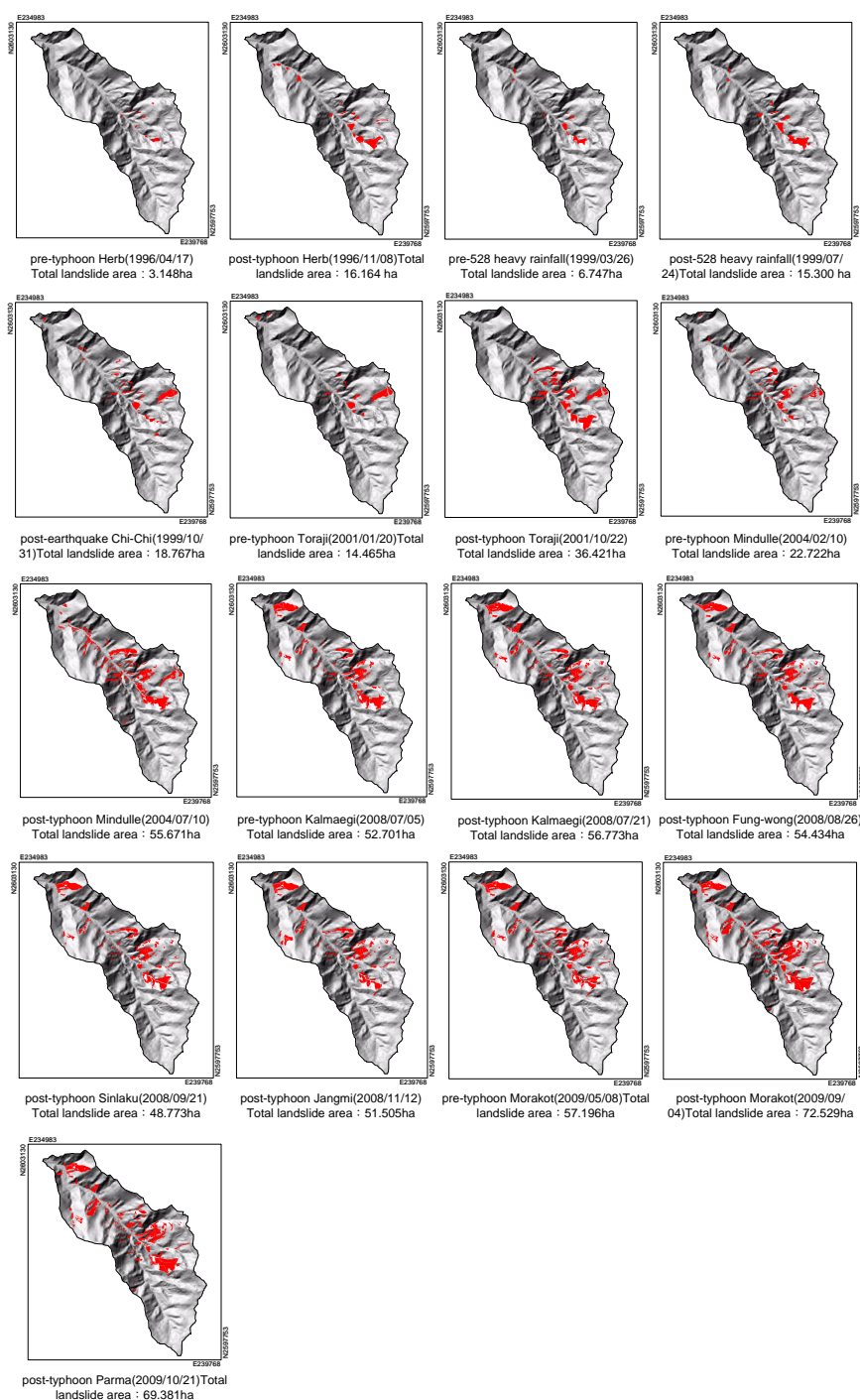
Figure 8. Landslide distribution of Chushui subwatershed for each event

2

Natural Hazards
and Earth System
Sciences

Open Access

EGU

Discussions
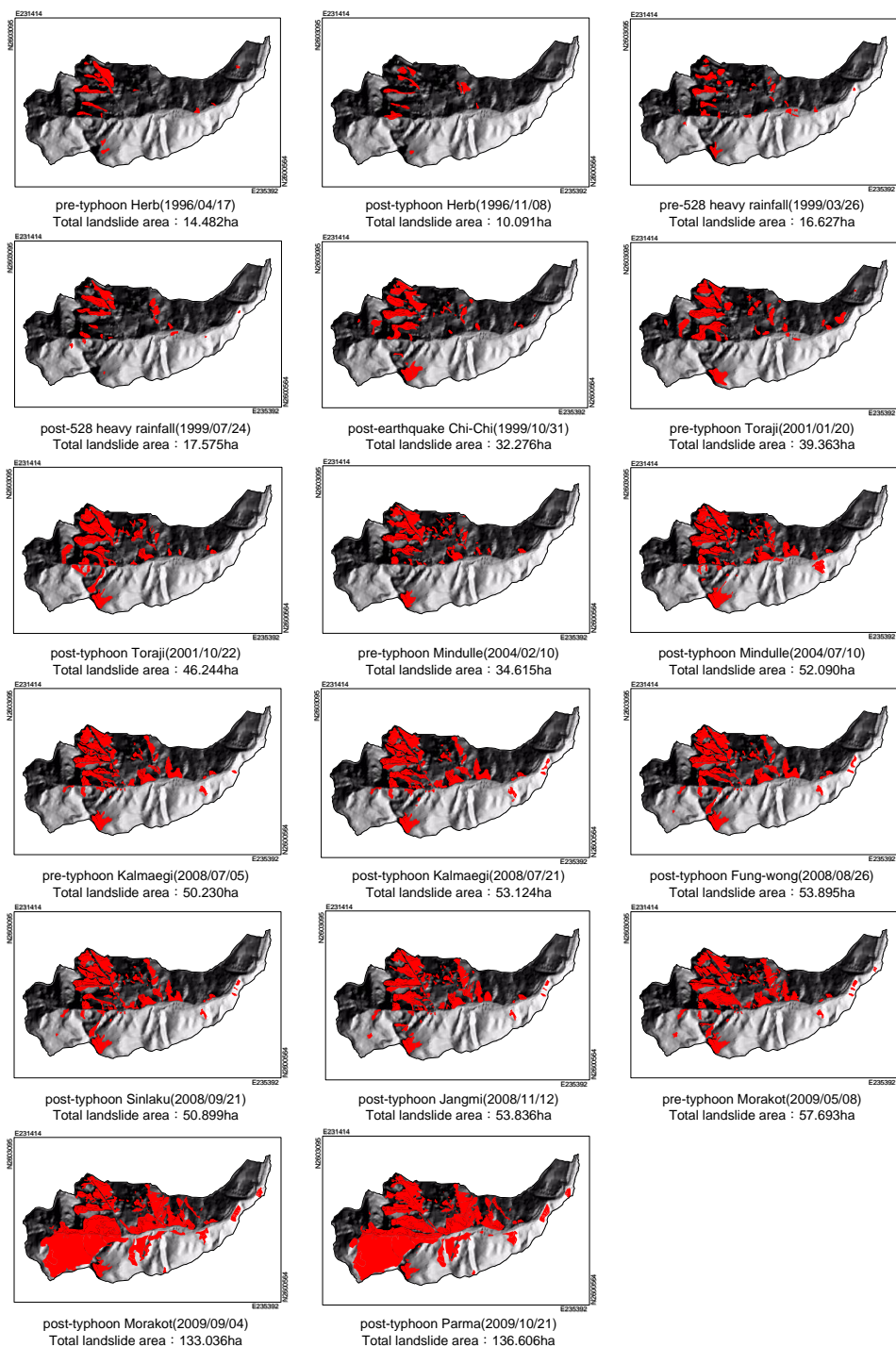
1

2   Figure 9. Landslide distribution of Aiyuzih subwatershed for each event

Natural Hazards
and Earth System
Sciences
Open Access
Discussions

EGU
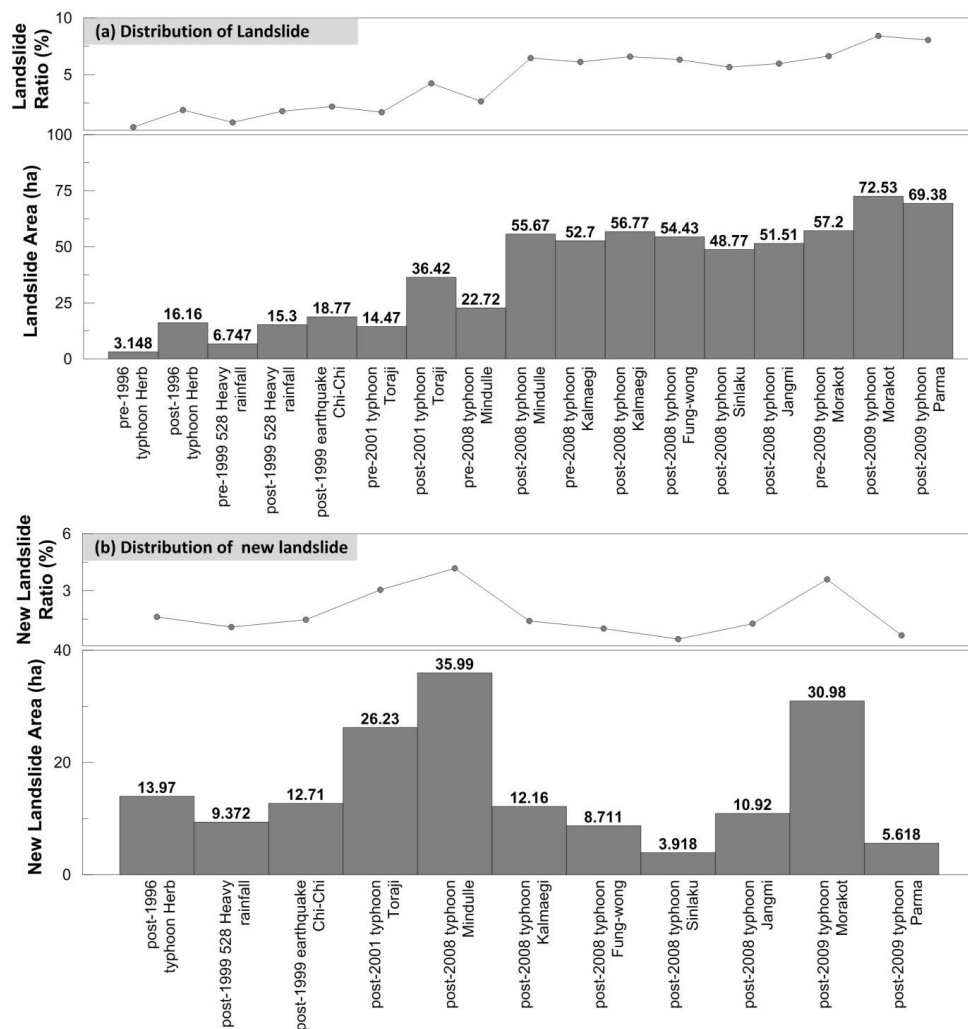
Figure 10. Landslide Distribution of Chushui subwatershed for each event in Temporal Scale

Natural Hazards
and Earth System
Sciences

Discussions
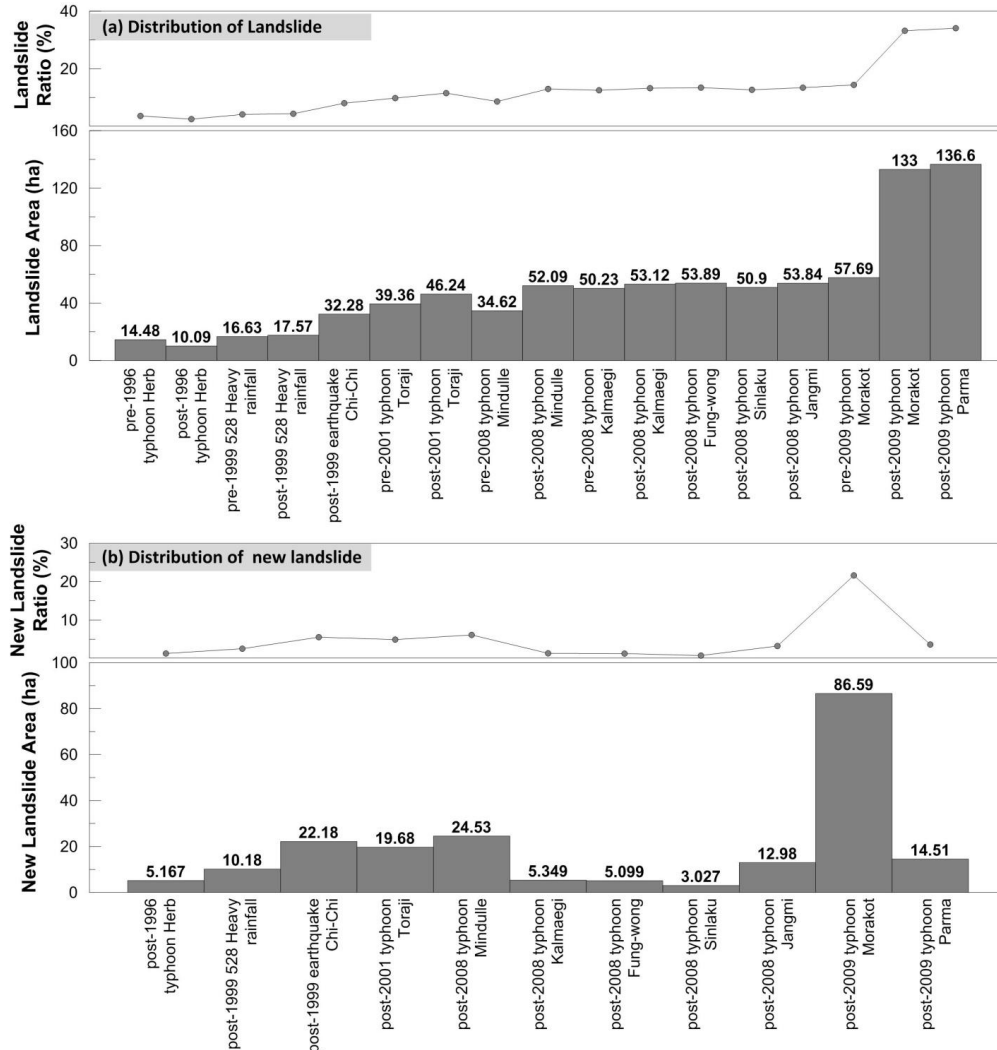
Figure 11. Landslide Distribution of Aiyuzih subwatershed for each event in Temporal Scale

1

2

3

4

5

6
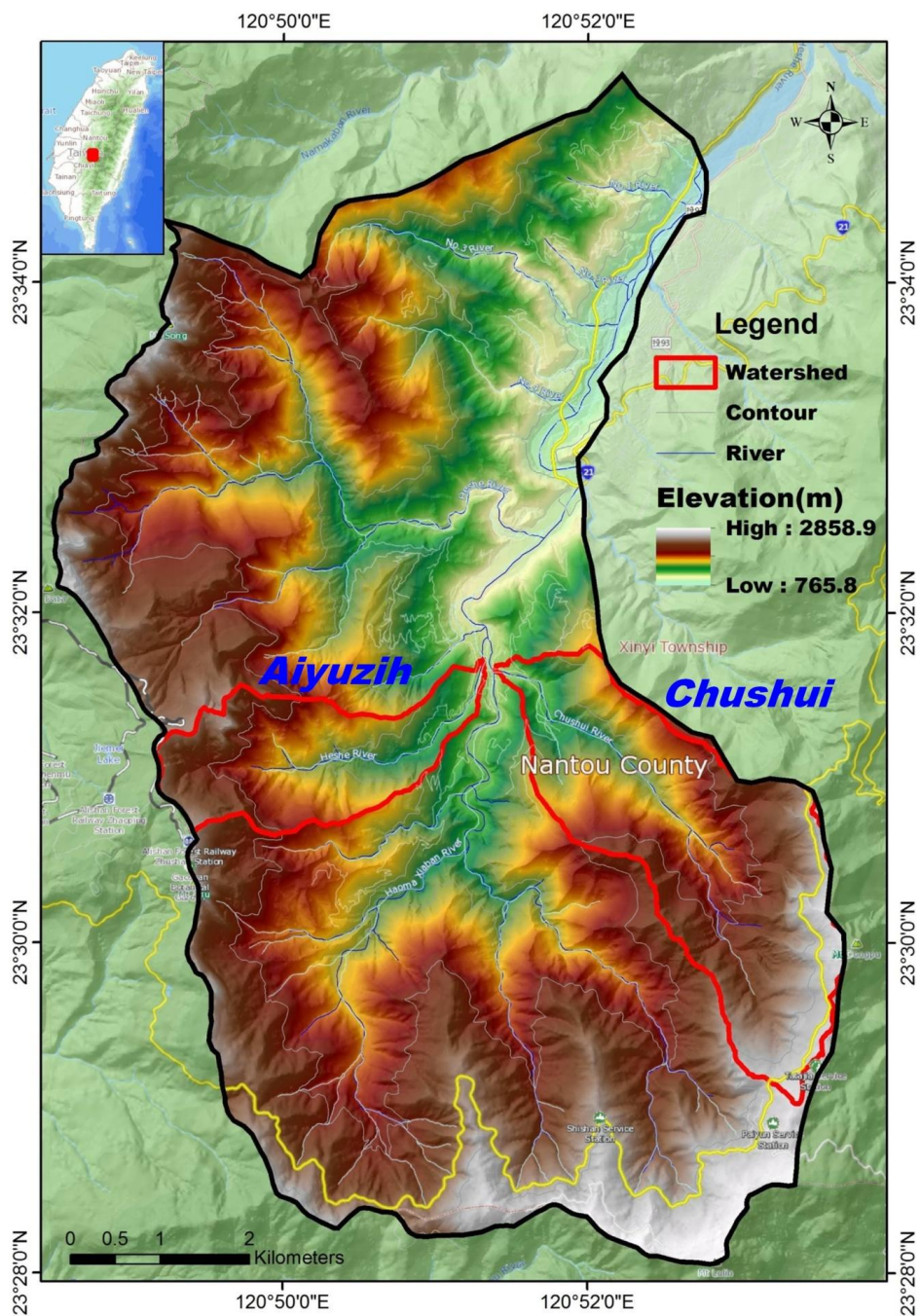
1
2   . Figure 12. 5mx5m DEM and terrain relief of the Shenmu watershed

3

Natural Hazards
and Earth System
Sciences
Open Access
Discussions
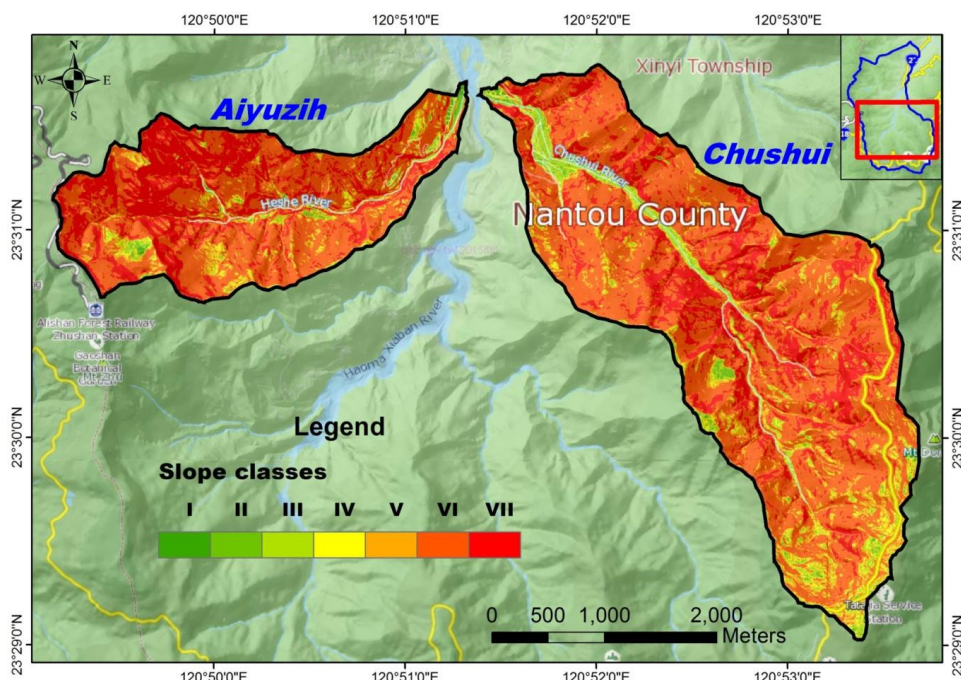
1

2   Figure 13. Slope map of Chushui and Aiyuzih subwatershed
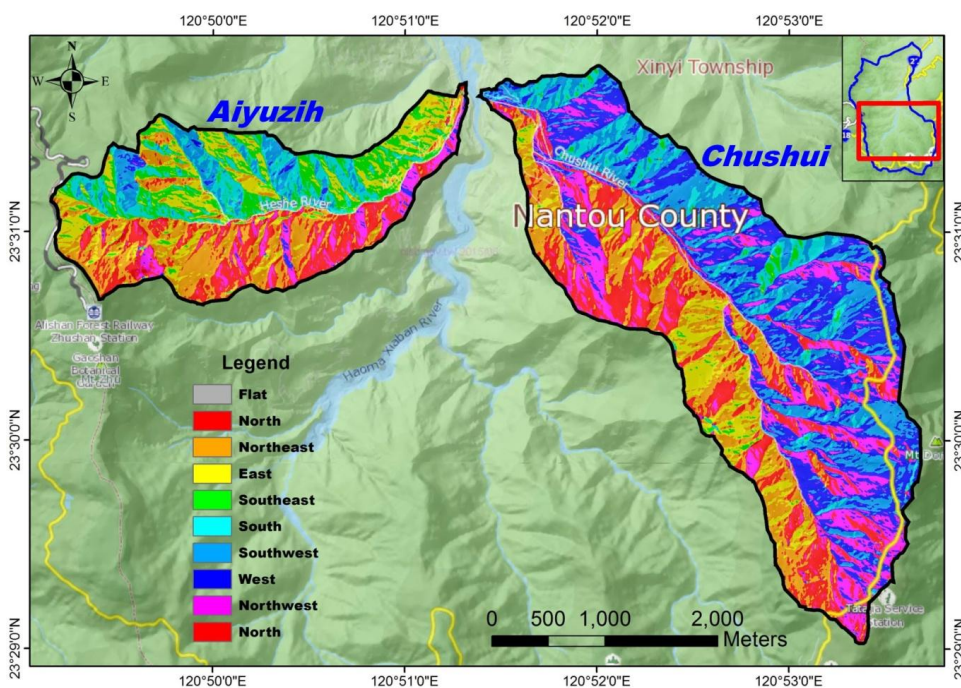
3

4   Figure 14. Slope aspect map of Chushui and Aiyuzih subwatershed

Natural Hazards
and Earth System
Sciences

Discussions

Open Access

1
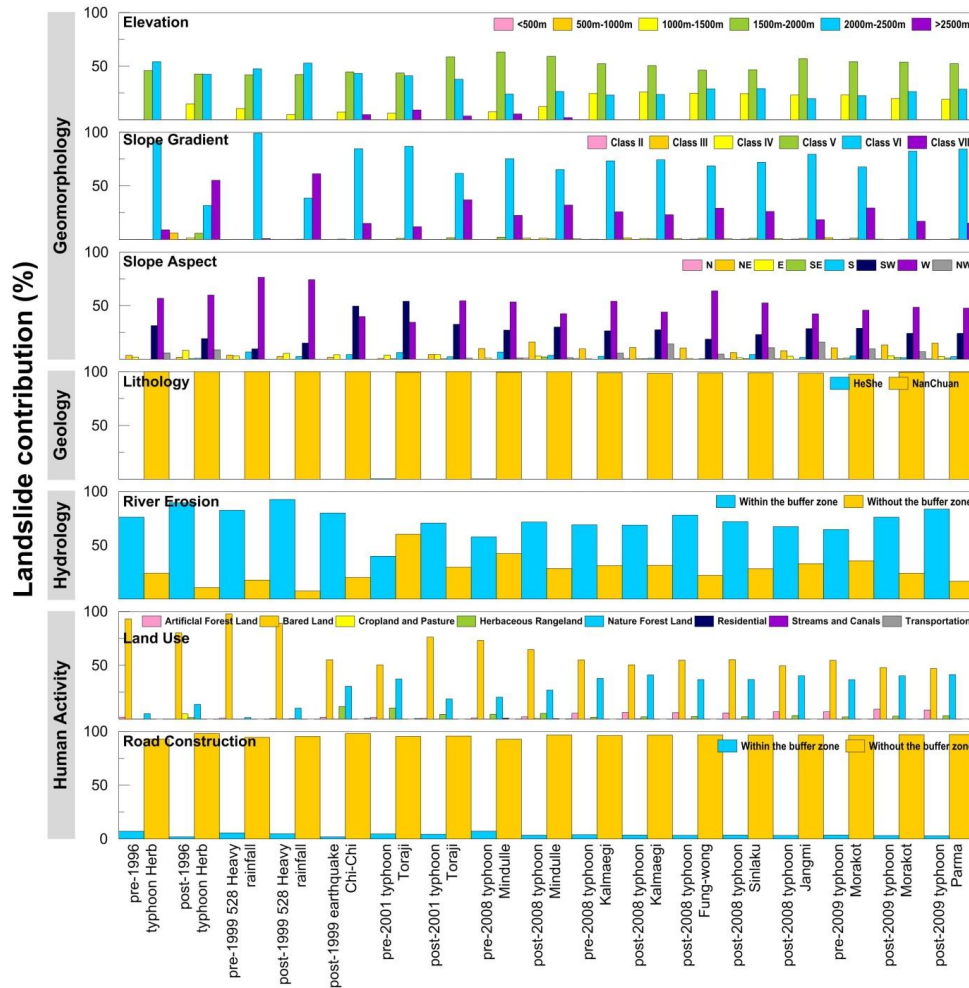
2   Figure 15. Landslide contribution (LC) of Chushui subwatersheds affected by environmental

3   factors

4

5

6

1
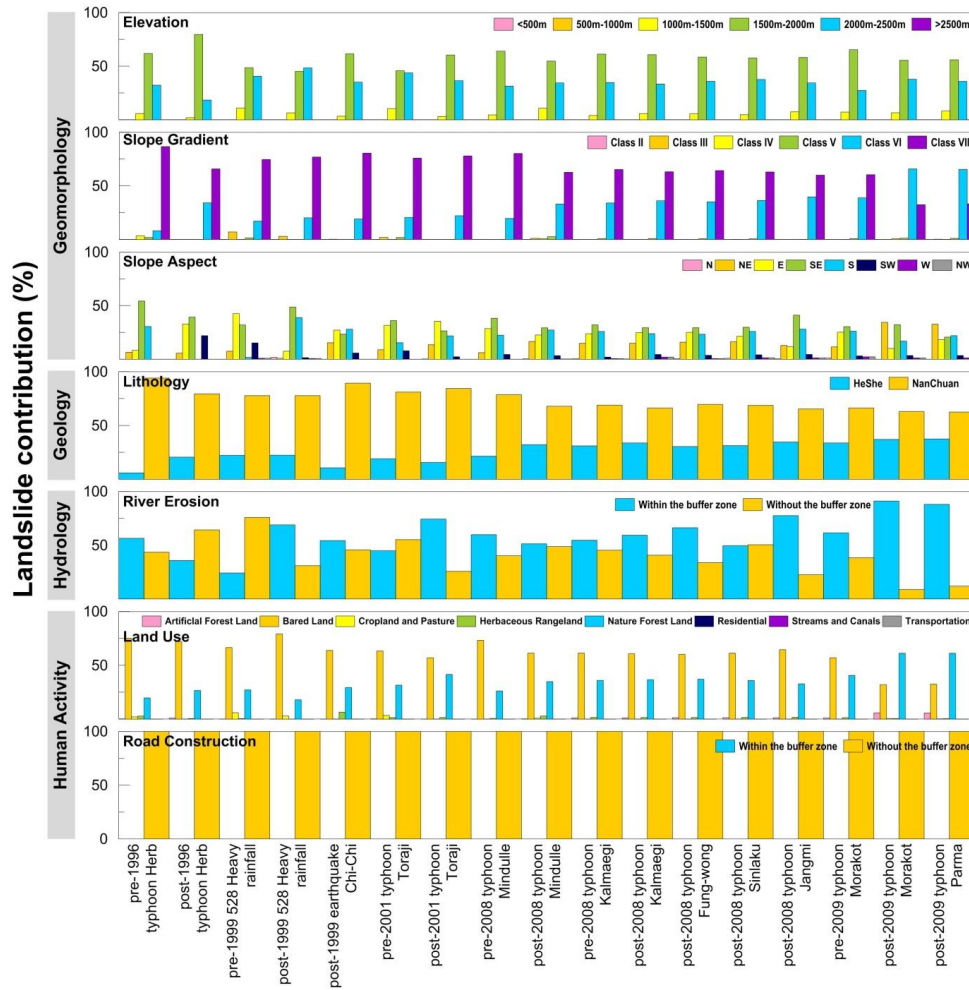
Figure 16. Landslide contribution (LC) of Aiyuzih subwatersheds affected by environmental

factors

4

5
6

Natural Hazards
and Earth System
Sciences

Open Access

Discussions

EGU

1
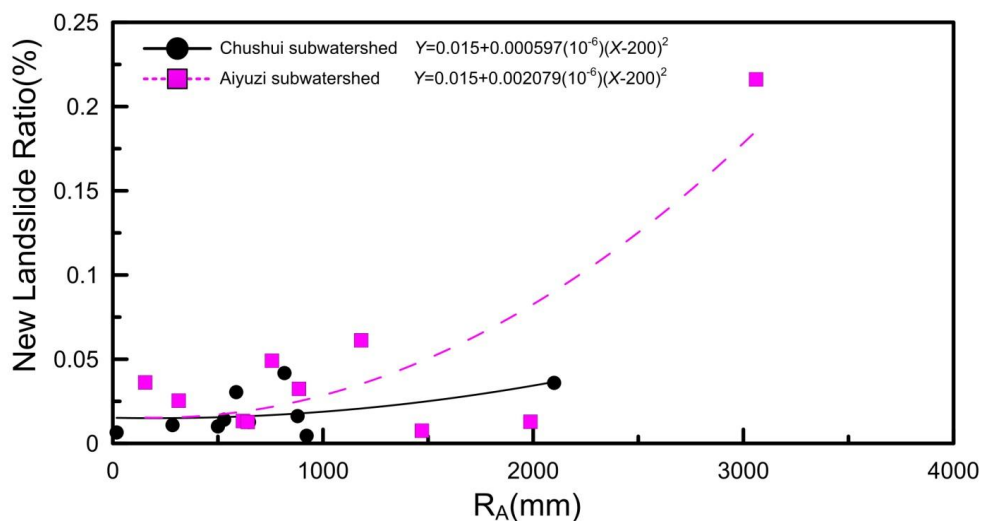
Figure17. Graph of the new landslide ratio of each event versus its corresponding

accumulated rainfall of Chushui and Aiyuzih subwatershed

4
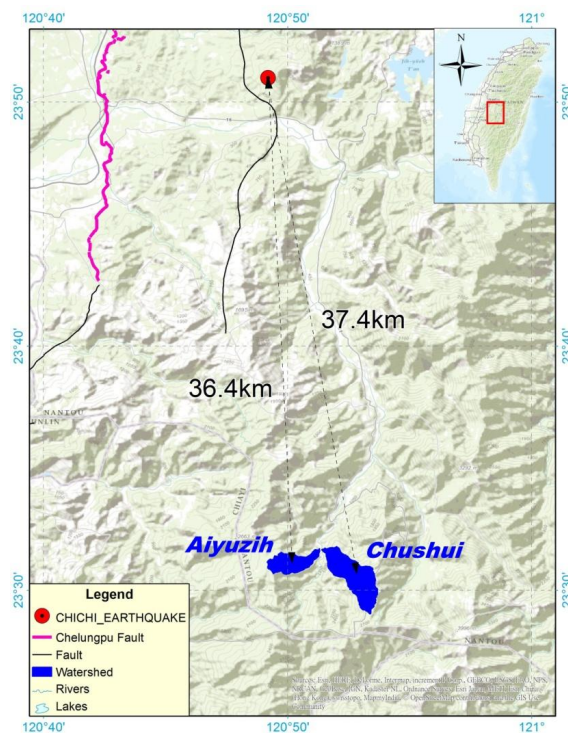
Figure18. Geographic maps of the distance from Chi-chi earthquake epicenter of Chushui and

Aiyuzih subwatershed

1
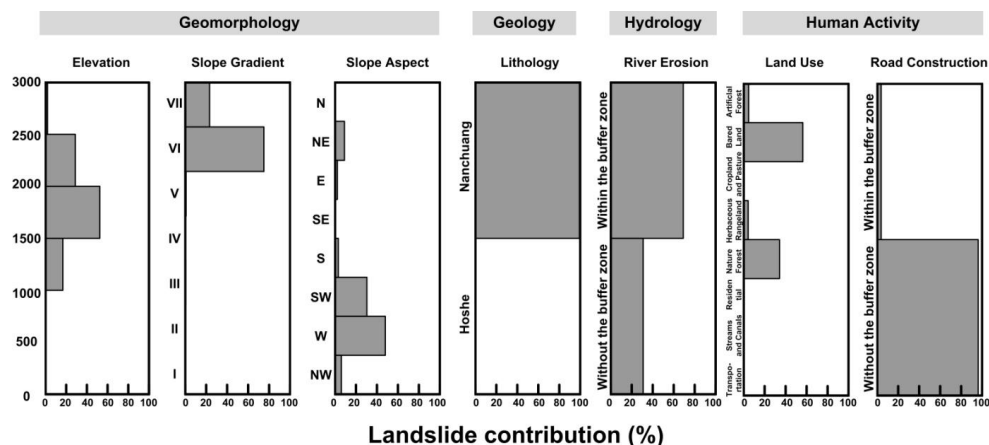
(a) Chushui subwatersheds
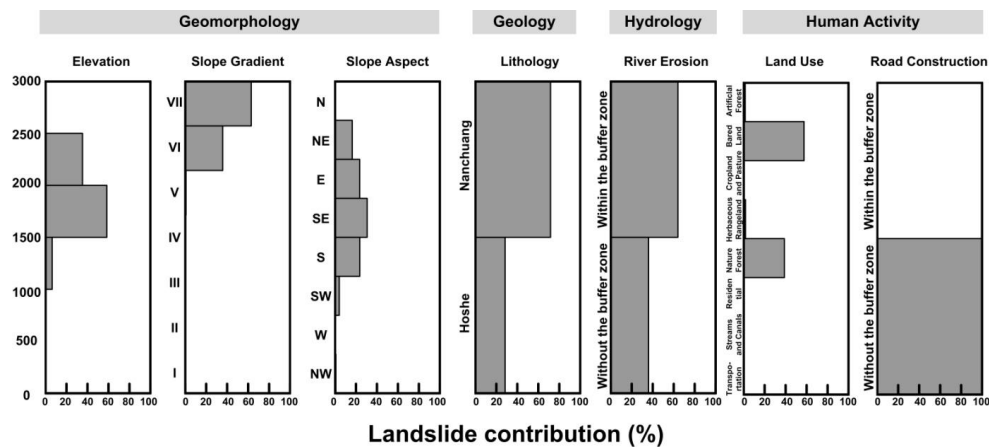
3
4   (b) Aiyuzih subwatersheds

5   Figure19. Graph of the average landslide contribution of various environmental factors after

6   1999 Chi-Chi earthquake for Chushui and Aiyuzih subwatersheds

Natural Hazards
and Earth System
Sciences

Open Access

Discussions

EGU

1
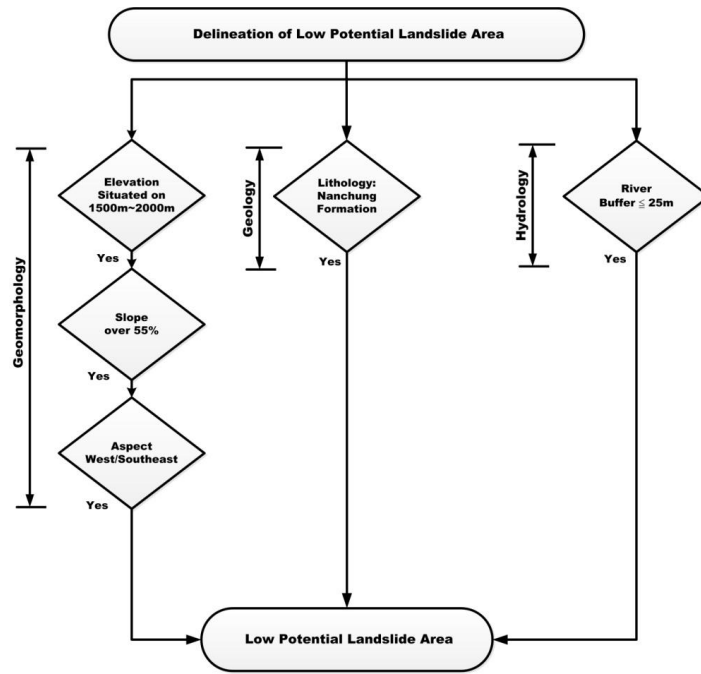
Figure 20. Procedure of delineation of low potential landslide area

3
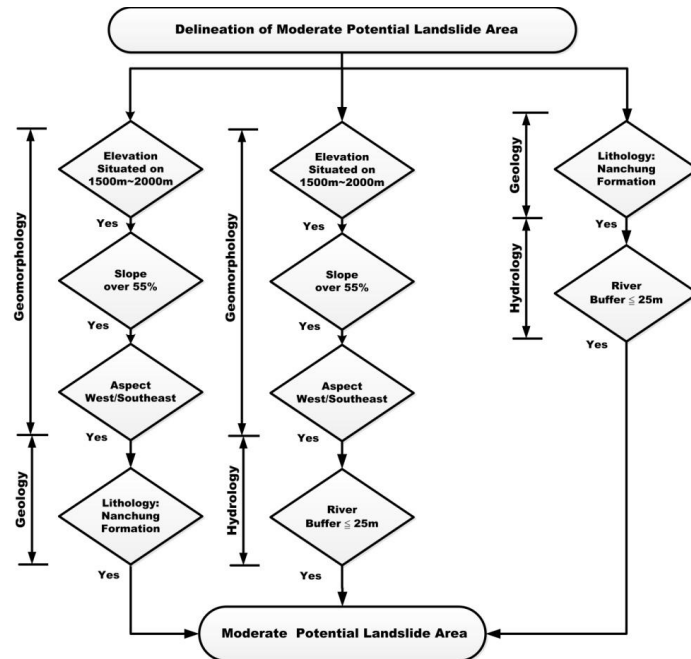
Figure 21. Procedure of delineation of moderate potential landslide area

1
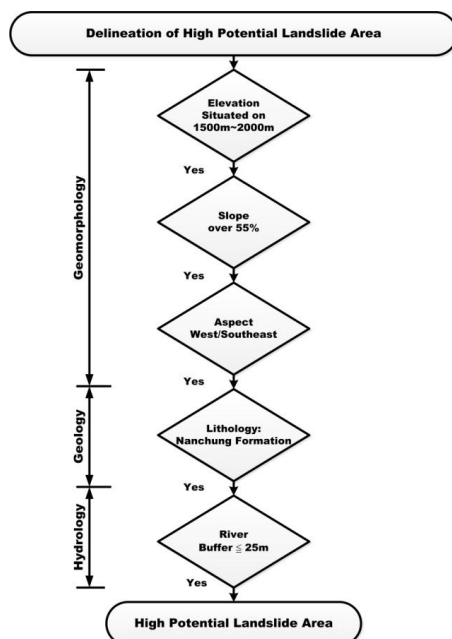
Figure 22. Procedure of delineation of high potential landslide area

3
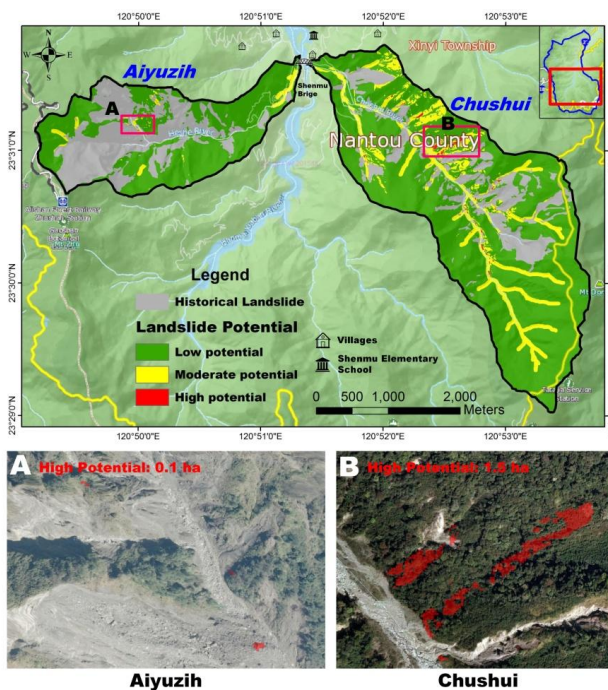
Figure 23. Landslide potential map of Chushui and Aiyuzih subwatersheds